TRANSITION FROM FILM BOILING TO NUCLEATE BOILING IN FORCED CONVECTION VERTICAL FLOW

Onwuamaeze C. Iloeje
David N. Plummer
Warren M. Rohsenow

Report No. DSR 72718-78

National Science Foundation
Contract No. NSF GK 17745

Engineering Projects Laboratory
Department of Mechanical Engineering
Massachusetts Institute of Technology
Cambridge, Massachusetts 02139

March 1972

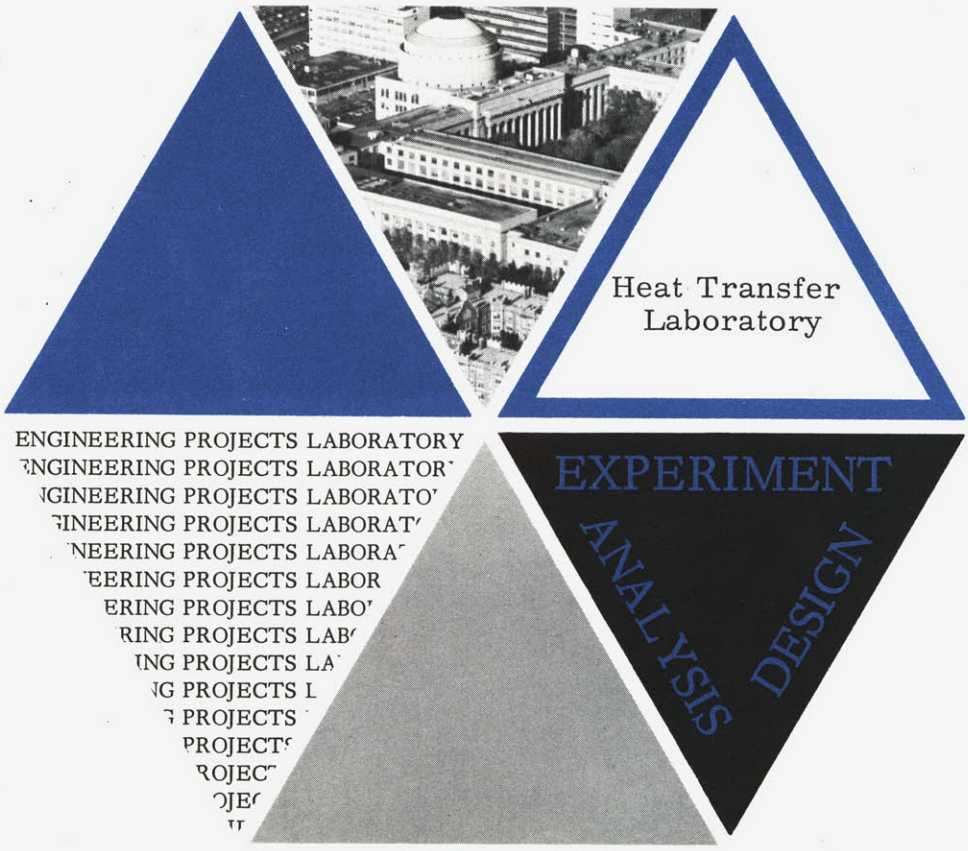

TECHNICAL REPORT NO. 72718-78

TRANSITION FROM FILM BOILING TO NUCLEATE BOILING IN FORCED CONVECTION VERTICAL FLOW

by

Onwuamaeze C. Iloeje

David N. Plummer

W. M. Rohsenow

Sponsored by the

National Science Foundation

Contract No. NSF GK 17745

DSR Project No. 72718

March 1972

Heat Transfer Laboratory
Engineering Projects Laboratory
Department of Mechanical Engineering
Massachusetts Institute of Technology
Cambridge, Massachusetts 02139

ABSTRACT

The mechanism of collapse of forced cnnvection annular vertical flow film boiling, with liquid core, is investigated using liquid nitrogen at low pressures. The report includes the effect of heat flux from the buss bar.

Tests include runs with mass fluxes varying from 44,000 lbm/hr-ft^2 to 186,000 lbm/hr-ft^2, and buss bar heat fluxes from 0 to 107,000 BTU/hr-ft^2. The channel was a 0.4 inch I. D. by 0.5 inch O.D. by 8 feet long Inconel 600 tube.

Two modes of collapse were isolated, in the absence of rewet by dispersed cooling within the mist flow region. These were axial conduction controlled collapse originating at the entrance to the test section for zero or negative buss bar heat flux; and impulse cooling collapse originating downstream of the entrance for heat into the test section from the buss bar. Collapse heat flux was found to be a function of mass flux, but the collapse wall temperature difference $(T_w - T_s)$ was independent of mass flux and could be successfully predicted within 6% by pool boiling minimum transition correlation (e.g. Berenson [5]).

ACKNOWLEDGMENTS

Support for this thesis was provided by the National Science Foundation. The authors are greatly indebted to Professors W. M. Rohsenow, B. B. Mikic, and P. Griffith for their invaluable suggestions, and to Mr. F. Johnson for his practical suggestions and work in modifying the apparatus. A special thanks goes to J. Horowitz for his contributions toward solving the numerous meddlesome problems encountered in this thesis.

TABLE OF CONTENTS

LIST OF FIGURES

NOMENCLATURE

h	heat transfer coefficient	BTU/hr-ft^2°F
D	cylinder diameter	ft
ϕ	as defined in eq. (1b)	
k	thermal conductivity	BTU/hr-ft°F
λ'	$hfg\ (1 + \frac{0.4\ C_v\ T_b}{hfg})^2$	BTU/lbm
ΔT_b	$(T_s - T_b)$	°R
h_{sg}	heat of evaporation	BTU/lbm
c	specific heat	BTU/lbm°F
ρ	density	lbm/ft^3
μ	viscosity	
σ	surface tension	
H	oscillating component of heat transfer coefficient	
δ	vapor film thickness	
t	time	
T	temperature	°R
y	film thickness	
y°	heat-up layer thickness	
T°	temperature at y°	
t°	time at y°	
P_s°	saturation pressure at T°	
P	pressure	
α	thermal diffusivity	

B_{WET}	$(T_{wet} - T_s)$	
B_i	$(T_i - T_s)$; i = 1, nucleate boiling side i = 2, film boiling side	
$\bar{h}$	mean heat transfer coefficient	
q	heat flux	BTU/hr-ft^2
q/A	heat flux	BTU/hr-ft^2
x	distance along insulator section	
r	radial dimension	
η_1	insulator thickness	
η_2	test section wall thickness	
z	distance along test section	
a	buss bar thickness	

SUBSCRIPTS

L or f	liquid
V	vapor
Vf	at vapor film temperature = $1/2(T_w + T_s)$
cb	contact boundary
Lo	initial liquid state
w	wall
e2	start of collapse
e1	end of collapse
$\overline{\quad}$	mean value
wet	at wetting conditions
c	thermodynamic critical state
s or sat	at saturation conditions
wo	initial wall state
$\langle\ \rangle$	time averaged value
BB or bb	buss bar
TS or ts	test section
*	corresponding to collapse

INTRODUCTION

A most important feature of film boiling is the characteristic low heat transfer coefficient compared with the heat transfer coefficients obtained in nucleate boiling. The ratio of forced convection nucleate boiling to film boiling heat transfer coefficients is of the order of 500 to 1000. The low coefficient is given rise to by the presence of a vapor film adjacent to the wall, with a heat transport mechanism less efficient than that for pool boiling.

In certain applications, as in nuclear reactors and once-through boilers, conditions of film boiling cause unusually high temperatures with likely metallurgical failure of the tubes. Both this fact and the low heat transfer coefficients demand that nucleate boiling be maintained, and regained should a power surge accident or coolant blockage cause burn-out. In order to incorporate this necessity into design and operational procedures, it is necessary that the mechanism of collapse be understood and the conditions be predictable.

In other applications, as in the transport of cryogenic liquids, it is desirable to maintain film boiling, with the film acting as an insulation to the liquid core.

Recent film boiling investigations [1] identified two regimes of film boiling: (a) Type I film boiling with dry wall starting from tube entrance; (b) Type II film boiling consisting of normal boiling with wet wall upstream. The report of reference [1] had indicated a strong effect of heat input from the electrical supply lead on the film boiling transition or collapse. This

report is concerned with the investigation of the mechanism of collapse of Type I film boiling, and the effect of heat flux from the buss bar, using liquid nitrogen in forced vertical flow.

The transition from film boiling to necleate boiling in forced flow has not been widely investigated, in contrast to the abundance of literature on the reverse problem of burn-out. Two major works are mentioned in this thesis - those of Kalinin [2], and Simon and Simoneau [3]. Their reports dealt with different theories of film boiling transition.

Finally, this report concludes with the statement that the temperature difference $(T_w - T_{sat})$ at collapse of film boiling in forced flow is not affected by mass flux. This suggests that it could be predicted by a pool boiling correlation, e.g. Berenson's [5], while collapse heat flux is a function of mass flux.

CHAPTER I

THEORIES OF FLOW FILM BOILING AND FILM BOILING COLLAPSE

1.1 Regimes of Film Boiling

1.1.1 Type I Film Boiling

The visual observations of Dougal [4] and others have established the existence of statistically stable annular film boiling starting from the heated tube entrance. Examination of the boiling curve (Figure 1) indicates that the heat flux and wall temperature levels must be set beyond the Leidenfrost (minimum heat flux) point before the passage of the liquid. The vapor flow within the annulus starts off initially laminar but quickly transits into turbulent flow within a short distance. Both within the laminar and turbulent regions, the vapor/liquid interface is wavy (Figure 2), possessing both transverse and time dependent large and small scale oscillations. A method of successful prediction of the amplitude of these oscillations does not as yet exist, and since the heat transfer coefficient depends on the film thickness, theoretical analysis for the prediction of the heat transfer coefficient, using various assumptions, have only met with limited success. Figures 3(a) and 3(b) illustrate the flow regime and a typical wall temperature profile.

Annular film boiling with a central liquid core can be assured with subcooled, saturated, or very low quality inlet for high Reynolds numbers at inlet, and low heat fluxes. It may be obtained at high heat fluxes, but the liquid Reynolds number will have to be low. It is easy to see that depending on the inlet subcool, flow rate, system pressure, and heat flux

level, the effect of the interfacial shear between the higher mean velocity and accelerating vapor, and the liquid, penetrates into the liquid core and changes the flow from fully separated to a dispersed mixture of vapor and liquid droplets of non-uniform sizes. The change of regime is expected to occur at a quality of about 10%. The liquid droplets, particularly the larger ones, are immediately projected towards the wall where they evaporate and cool the wall in the process. The dispersed boiling process is accompanied by the formation of a vapor film which is initially unstable, but evantually becomes stable as the droplet sizes decrease.

1.1.2 Assumptions in the heat transfer analysis of annular vapor film boiling

1.1.2(a)

The first partially successful analysis of film boiling from horizontal cylinders was by Bromley [6]. Interfacial waves were not accounted for, and a laminar film was assumed. The resulting expression was of the form:

$$h = 0.62 \left(\frac{\phi}{D}\right)^{1/4} \tag{1a}$$

where

$$\phi = \frac{k_g^3 \lambda' C_g (\rho_i - \rho) \rho g}{\mu_g \Delta T_b} \tag{1b}$$

1.1.2(b)

Berenson [5] applied the Taylor instability concept to a horizontal plate. The resulting expression for heat transfer coefficient at collapse was of the form:

$$h = 0.62 \left[\frac{k_{vf}^3 \lambda' \rho_{vf} g (\rho_\ell - \rho_v)}{\mu_f \Delta T\, d}\right] \quad ; \quad d = \left[\frac{g_o \sigma}{g(\rho_\ell - \rho_v)}\right] \tag{2}$$

1.1.2 (c)

Dougal and Rohsenow [4] analyzed the vapor film, assuming it to be a two-dimensional flow between a plane wall and a plane liquid/vapor interface, although film thickness at any given position varied.

The universal velocity distribution was used to solve the momentum and heat transfer equations in turbulent flow. He found that his data for Nusselt numbers could be correlated better by assuming the thermal resistance of the interface half of the vapor film to be that due to a fully turbulent vapor layer, particularly at high vapor Reynolds numbers. This was an indirect way of accounting for the increased heat transfer which would be obtained in an analysis incorporating interface oscillations, instead of using a mean film thickness.

1.1.2(d)

G. E. Coury and A. E. Dukler [7] performed a vapor film analysis that attempted to take account of the large scale interface oscillations. The motion of the interface was modelled as a quasistatic wavy profile upon which was superimposed a time dependent local variation in film thickness. A non-symmetric velocity profile (Figure 4) was assumed, and the turbulent momentum and energy equations were solved numerically by a matching process. From this, local quasistatic Nusselt numbers were found as functions of film Reynolds numbers. Then the Nusselt numbers were assumed constant with time so that

$$Nu = \frac{h(t)\ \delta(t)}{k_v} = \frac{h_s \delta_s}{k_v} \qquad (3)$$

h_s = quasistatic local heat transfer coefficient

$h(t)$ = time dependent heat transfer coefficient

Also $h(t)$ was assumed to be sinusoidal and equal to $\langle h \rangle_t + H(t)$ so that

$$\frac{\langle h \rangle}{h_s} = 1 + \frac{\langle H^2 \rangle_t}{\langle h \rangle_t^2} \qquad (4)$$

The ratio $\frac{\langle H^2 \rangle_t}{\langle h \rangle_t^2}$ was determined from experiment. Thus the effect of interface oscillations still requires to be experimentally found.

1.1.3 Type II film boiling

For this case, normal nucleate boiling incorporating the various regimes up to dryout exists upstream, side by side with dispersed film boiling downstream. This regime is not of central interest to the thesis, for it can be argued that nucleate boiling occurring side by side with dispersed film boiling in the same uniformly heated tube implies that collapse had already occurred. If the vapor/liquid interface was in equilibrium at any set of conditions of heat flux and wall temperature profile, such an equilibrium is very unstable, as mathematically demonstrated by Semeria and Martinet [3]. (Experiment showed that a small reduction in heat flux, for example, was sufficient to cause the interface to propagate downstream. Figures 5(a) and 5(b) indicate the flow regime and a typical wall temperature profile.)

1.2 Theories of Collapse

1.2.1 Impulse Cooling Collapse

Liquid in contact with a hot wall at a temperature $T_w > T_{wet}$ will remain in film boiling until the wall temperature has been cooled to or below the wetting temperature. It has been postulated that T_{wet} is equal to the

maximum superheat of a liquid and hence is a unique function of the thermodynamic state. Using van der Waals' equation of state, Spiegler et al. [9] obtained an expression for the minimum film boiling temperature as a function of the critical state and liquid pressure.

$$\frac{T_{WET}}{T_c} = 0.13\frac{P}{P_c} + 0.84 \qquad \text{for } \frac{P}{P_c} > 0.07 \tag{5}$$

Merte and Clark [10] have reported a wetting temperature difference $(T_{wet} - T_s)$ for liquid nitrogen of 33.4°K at 1 atmosphere. Kalinin et al. [11] used a value of T_{wet} for liquid nitrogen at 5 atmospheres of 114°K.

The postulate for collapse used in [2] and [11] envisaged that as the wall temperature fell, the film thickness decreased and would eventually become small enough that crests of the liquid/vapor wavy interface would start to hit the surface. As the liquid hit the surface, the contact boundary would immediately attain a temperature T_{cb} given by

$$\frac{T_{cb} - T_{Lo}}{T_{wo} - T_s} = \sqrt{\frac{(k\rho C)_w}{(k\rho C)_L}} \tag{6}$$

One of three things would occur. If $T_{cb} > T_{max}$, the temperature of maximum metastable superheat of the liquid, a very rapid and vigorous evaporation would occur. If $T_{cb} < T_{max}$, the liquid would remain in contact with the wall for a period t°, sufficient to heat up a layer of fluid of thickness y° , equal to the minimum diameter of equilibrium vapor nucleus, given by

$$y^\circ = \frac{4\sigma^\circ}{P_s^\circ - P_L} = f(T^\circ) \tag{7}$$

to its superheat temperature T°.

Vapor may then nucleate. If $T°$ is not achieved, the liquid will remain in contact with the wall and collapse would have occurred. Usually it will take repeated contacts of crests of liquid waves before collapse can occur.

In reference [2], Kalinin et al. performed a conduction analysis to obtain the liquid temperature as a function of distance y into the liquid, and time, treating the liquid at a semi-infinite stationary medium at an initial uniform temperature T_{LO} and the wall as a flat, unheated plate of thickness δ_w and initial temperature, T_{wo}. The result was

$$\frac{T_L(y,t) - T_{Lo}}{T_{wo} - T_{Lo}} = \frac{1}{1 + \sqrt{\frac{(k\rho c)_L}{(k\rho c)_w}}} \left[\operatorname{erfc} \frac{y}{2\sqrt{a_L t}} - \frac{2}{1 + \sqrt{\frac{(\rho c k)_w}{(\rho c k)_L}}} \operatorname{erfc}\left(\frac{y}{2\sqrt{a_L t}} + \frac{\delta_w}{2\sqrt{a_w t}} \right) \right] \quad (8)$$

Using eq. (7) and (8) and the condition that at $t°$ and the corresponding values ot $y°$ and $T°$, the rate of change of temperature with time is a minimum and equal to zero,

$$\left(\frac{dT}{dt} \right)_{y°} = 0 \quad (9)$$

It is possible to graphically solve for $y°$, $t°$, $T°$. With these the liquid temperature $T(0, t°)$ can be found from eq. (8). This also equals the wall temperature. However, in order that the solution may be directly useful, the number of collisions before collapse - in effect the interfacial wave structure as well as the temperature recovery magnitude of the wall after each collapse - need to be known. The lack of such information would appear to make eq. (8) useless. However, it served the purpose of indicating the dependence of the temperature at start of collapse on the ratio

$$\sqrt{\frac{(k\rho c)_L}{(k\rho c)_w}}$$

As the film thickness fell, the frequency of liquid contact increases and the contact period also increases with the result that the rate of change of wall temperature with time would experience a minimum. This corresponds to the start of collapse. The end of collapse is characterized by the point at which the rate of fall of temperature with time is maximum, and shows as an inflection point in the temperature-time plot. The corresponding temperatures are denoted by Te_2 and Te_1.

Curves of $\frac{Te_1 - T_s}{T_c - T_L}$ vs. $\sqrt{\frac{(k\rho c)_L}{(k\rho c)_w}}$ gave the following empirical relationships for both free and forced convection

$$\left(\frac{Te_1 - T_s}{T_c - T_L}\right) = 0.1 + 1.5\left[\frac{(\rho c k)_L}{(\rho c k)_w}\right]^{.25} + 0.6\left[\frac{(\rho c k)_L}{(\rho c k)_w}\right] \tag{10}$$

$$\left(\frac{Te_2 - T_s}{Te_1 - T_s}\right) = 1.65 \tag{11}$$

for $0.03 \leq p/p_c \leq 0.65$ and contact angles approximately equal to zero.

The terms above used in plotting the graphs do not derive logically from their solution of the conduction model.

1.2.2 Axial conduction controlled collapse

Nucleate boiling occurring side by side with film boiling creates an axial temperature gradient within the walls of the material. Semeria and Martinet [8] performed an analysis on the propagation, stability, and resorption of a calefaction spot on a heated wall. By assuming constant heat transfer coefficients and temperatures on the film boiling and nucleate boiling sides they arrived at the relation

$$B^2_{WET} = (B_1)(B_2) \tag{12}$$

for the condition that velocity of propagation of the interface is zero. This would correspond to the instant of formation of the spot at some equilibrium state.

The theory and analysis of Simon and Simoneau [3] is based on the assumption that for a constant heat flux wall, when nucleate and film boiling occur side by side, the transition heat flux is governed by axial condiction within the wall, from the film to the nucleate boiling sides. The control is effected by the conduction process being able to cool down the leading edge of the film to a value which will permit liquid wetting of the metal surface. They made a slight modification to eq. (12). B_1 and B_2 were defined as the average heat transfer coefficients for nucleate and film boiling.

$$B_{WET}^2 = \left[B_1, \bar{h}_1\right]\left[B_2, \bar{h}_2\right] \tag{13}$$

Eq. (5) gave a relation for B_{wet}.

The forced convection component of nucleate boiling heat transfer was ignored so that using Kutaleladze correlation for pool boiling heat transfer

$$q_{Pb} = 4.87 \times 10^{-7} \left(\frac{c_L}{h_{fg}}\right)^{1.5} \left(\frac{k_L \rho_L^{1.282} P^{1.75}}{\sigma^{.906} \mu_L^{.626}}\right) B_1^{2.5} \tag{14}$$

they eventually obtained for $B_{1,\bar{h}}$ that

$$B_{1,\bar{h}} = \frac{B_1}{1.84} = f(P, q, \bar{u}_L) \tag{15}$$

B_1 is obtained from pool boiling data or correlation.

Using eq. (13) and (15), $B_{2,\bar{h}}$ may be found for various values of heat flux, from which can be plotted curve EF in Figure 1. An expression for the boiling curve region CD was obtained by assuming laminar film boiling with additional correction for the waviness of the interface. This was given by

$$\left(B_{2,\bar{h}}\right) = X \Big/ \left[\tfrac{5}{4} a_1 \left(B^4 - B_{wET}^4\right) + \tfrac{4}{3} a_2 \left(B^3 - B_{wET}^3\right) + \tfrac{3}{2} a_3 \left(B^2 - B_{wET}^2\right) + 2 a_4 \left(B - B_{wET}\right) + a_5 \ln \frac{B}{B_{wET}} \right] \tag{16}$$

The a's are constants depending on heat flux, saturation temperature, pressure, thermophysical properties of liquid and vapor, and ϵ defined as $\frac{\delta_L}{\delta}$ (see Figure 2). A graphical solution of eq. (13), (15), and (16), i.e. intersection of CD and EF on the boiling curve, was deemed to give the dry wall temperature difference and the corresponding heat flux.

They concluded that by the use of values of ϵ between 0.6 and 0.3 in a matching process for various velocities between 1 m/s and 2.5 m/s they were able to make the analysis fit the experiment, for the $(T_w - T_s)$ profile. Prediction for the variation of the transition heat flux with velocity at various pressures was not successful, but only indicated the expected trend.

The model they used did not take into account the discontinuity in heating in the power inlet rod/test section combination. The most likely position of the liquid/vapor/wall interface prior to collapse, with Type I film boiling and no radial buss bar heat flux, is just upstream of the point of discontinuity and not within the uniformly heated test section, as their model assumed. The latter case would imply that collapse had already occurred. The justification of using mean film boiling and nucleate boiling heat

transfer coefficients to describe the local phenomenon of annular film boiling collapse is not very attractive. The results they obtained could not therefore have been expected to agree with the data.

1.2.3 Dispersed cooling rewet

Within the region of dispersed flow boiling the droplets hitting the wall at various angles of attack may by repeated cooling impulses reduce the wall temperature to just below the wetting temperature, thereby causing rewet. For the case of the uniformly heated tube, such a mode of rewet was not observed. Keeys et al. [12] observed the rewet mode of collapse with a cosine heat flux distribution. The controlling process here will be heat transfer to a drop projected against the wall from the free stream, as well as the frequency of drop arrival at the wall and drop contact time. This mode of collapse is expected to hold for qualities of about 10% and over.

CHAPTER II

EXPERIMENTAL PROGRAM

2.1 Description of Apparatus

The experimental apparatus for this program was originally constructed by Laverty, later modified first by Forslund then Hynek. A schematic diagram of the apparatus is given in Figure 6. Liquid nitrogen is forced out of either one or two 160 liter Dewars (Linde LS-160) by a constant pressure head of 100 PSIG supplied by a regulated high pressure gaseous nitrogen supply. The liquid nitrogen is then led by means of 3/8 in copper tubing through two precoolers, through a flow control valve into the test section. The standard 22 PSIG relief valve of the Dewars had to be replaced with a 100 PSIG relief valve. The higher pressure in the flow line allowed the capacity of severe throttling at the inlet, thus helping to control one type of flow oscillation. The precoolers allowed the variation of inlet subcool and also prevented flashing at the flow control valve.

In the vertical test section, consisting of a circular insulated tube, direct resistance heated, the pressure is monitored by five pressure taps in conjunction with a manometer board. The tube wall temperatures were measured by copper-constantan thermocouples spot-welded to the tube. The fluid inlet temperature was measured by a shielded thermocouple in the liquid stream. The thermocouple was specially calibrated for liquid nitrogen temperatures as the standard thermocouple tables are not accurate at these low temperatures. This was done by placing a vessel containing liquid nitrogen in a bell jar

and reducing the pressure incrementally. When the liquid nitrogen boiled, the output of the thermocouple immersed in the liquid was recorded and plotted as saturation temperature for the particular pressure in the system (Figure 7).

The flow once through the test section is led through either one or two heat exchangers to evaporate the remaining liquid and to raise the gas temperature to around room temperature before entering the flow measuring device (rotometer). The gas is then exhausted into the atmosphere. More detailed discussion of the apparatus can be found in [13] and [1].

2.2 Modification and Improvements

2.2.1 Test section

The test section was the same tube used by Hynek [1] and consisted of an inconel 600 tube 0.4 inch I.D. by 0.5 inch O.D. and 8 feet long. The major modifications in the test eection consisted of rearranging the spacings of the wall thermocouples, modifying the type of insulation, and redesigning the lower buss bar. The last modification will be discussed in the next section. As for the thermocouple positions, Hynek spaced the thermocouples at four-inch intervals over the length of the tube. In this program it was supposed that collapse would occur at or near the entrance of the test section. To record the phenomenon more fully, it was necessary to space thermocouples at approximately one-inch intervals for the first ten inches, at the same four-inch intervals for the remaining length of the tube. The thermocouple positions are shown in Figure 8.

In the first stages of assembling the test section, it was found that Hynek had a converging nozzle coupler that allowed him to attach the test section to the delivery tube which was of slightly larger diameter. As it was felt that having this nozzle type flow pattern at the inlet to the test section might have an effect on the collapse mechanism, an inlet length of stainless steel tubing of the same I.D. as the test section was added to the delivery tube before the test section inlet. The test section was insulated electrically and thermally from the delivery tube by a micarta spacing. For a ΔT drop of $400°F$ across the spacer, the heat loss was calculated to be 1 BTU/hr, allowing the assumption of zero heat loss from the test section inlet down through the delivery tube.

The Santocel insulation that Hynek used was discarded for safety reasons. Frequent disassemblies of the test section caused large amounts of the very fine Santocel dust to float into the air, thereby making it unsafe to breathe without a filter mask. Instead, blown mica called vermiculite was placed in the plexiglass shell surrounding the test section. As an added heat loss shield, layers of fiberglass blanket insulation known as aircraft insulation were wrapped around the outside of the plexiglass shell. Tests were run to determine heat loss (see Appendix A).

2.2.2 Buss Bar Heat Exchanger

Hynek in his experiment noted that there was a large heat flux into the test section through the electric power leads. To negate this flux he installed a guard cooler to the buss bar. The cooler, due to lack of control, succeeded

only in reversing the flow of heat from in to out of the test section. Therefore a redesign of the buss bar was necessary due to the assumption that axial conduction is a prime variable in the collapse mechanism.

Incorporating into the design as much control versatility as possible meant being able to control heat into and out of the test section. The magnitude of the heat flux as well as the control capability had to be such that zero heat flux conditions as well as specified heat flux in or out through the buss bar could be maintained during the data run.

The resulting heat exchanger-buss bar combination that was used is shown in Figure 9. It was constructed from solid copper rod 2 inches in diameter by 7 inches long. The system provides a means of piping liquid nitrogen from the main Dewar through a control valve into the main cylindrical area of the buss bar in which twenty 3/16 inch holes were axially drilled. The fluid was then exhausted into the vacuum system. As an extra control device, a second valve was placed between the heat exchanger exit port and the vacuum line. This part of the design allows heat outflow.

To affect heat flux into the test section, 1.1 ohm Cromel resistance wire electrically insulated with glass sleeving was tightly wrapped around the cylindrical section to form the heater element. This layer of wire was then coated with a liquid porcelain. This coating keeps the resistance heater in place. The heater was regulated with a 110 Volt ac variable auto-transformer.

To measure the heat flux, four copper-constantan thermocouples were inserted into four holes the size of a thermocouple bead spaced 0.25 inches apart along the axis of the bar as shown in Figure 9. The two thermocouples spaced near the test section were used to determine zero heat flux. The buss

bar apparatus was then silver soldered into place at the test section inlet as shown in Figure 8. The three bolts used to anchor the test section to the delivery tube were insulated from the buss bar with micarta sleeves. The entire buss bar assembly was insulated in the same manner as the test section.

The maximum heat flux into the test section from buss bar was on the order of 100,000 BTU/hr-ft^2 . The buss bar temperature necessary to give this heat flux is near the melting point of the glass sleeving used to insulate the wire. In one data run the heater did fail as the temperature reached 600°F . The full capacity of the cooler to draw heat out was never used as a very small valve setting was more than enough to cool the buss bar. In fact, most runs had to employ both the heater and the cooler when small heat fluxes out or zero heat flux conditions were desired.

2.3 Instrumentation and Accuracy

2.3.1 Thermocouple measurement

The first eleven thermocouples on the test section were recorded on a Honeywell Speedomax W 24 point recorder. This instrument was selected for its high cycle time of 1.2 seconds per point. The recorder was modified to read only 12 channels which gave a total time to read 12 thermocouples of 14.4 seconds. As the collapse mechanism occurred in a time period of about one minute, this instrument was well capable of recording wall temperature-time history of the collapse.

The specified accuracy of the instrument by the company is at least $\pm$ 0.3% of full scale, which for this set-up was 24 millivolts. Therefore the millivolt output was accurate to $\pm$0.07 mv or $\pm$ 4°F . The instrument was calibrated and found to be much better than the instrument specifications. The largest error came from the interpolation of the data points from the recording charts. The chart can be read only to $\pm$ 0.05 mv which gives a $\pm$ 3°F error for wall temperature. The inner wall temperature formula is derived in Appendix A.

The inlet fluid temperature thermocouple was read on a Leeds and Northrup Precision Potentiometer, which could be read to $\pm$ 0.005 mv, or $\pm$ 1/4°F. The instrument was calibrated to within these limits.

The remaining twenty thermocouples were connected through a switching network to a Brown 16-channel recorder (Minneapolis Honeywell Model 153X52U16). This instrument was calibrated to $\pm$ 0.05 mv. The data taken from these thermocouples were only to indicate if the collapse occurred at a position away from the inlet. As this never occurred for the uniform heat flux test section, the data was not used.

The six thermocouples on the buss bar were monitored through the Brown recorder. All data points used to calculate buss bar heat flux were recorded from the precision potentiometer. The accuracy is estimated to be of the order of $\pm$ 500 BTU/hr-ft^2.

2.3.2 Test section heat flux

The test section voltage was measured by a standard a-c panel voltmeter 0-15 volt scale. The secondary current was measured by a standard a-c panel ammeter 0-5 amperes scale. The combined calibration and interpolation error

for the voltmeter and the ammeter is $\pm$ 0.25 volts and $\pm$ 0.05 amperes, respectively.

The heat loss from insulation was experimentally obtained by a method described in Appendix A. The heat addition through the insulation at collapse was determined to be approximately equal to 300 BTU/hr ft^2. The total uncertainty of the minimum heat flux is approximately $\pm$ 100 BTU/hr-ft^2.

2.3.3 Flow rate

The flow rate was measured by two rotameters in parallel. The flow meters were calibrated using water as the calibration fluid. Assuming that the flow meter is independent of viscosity, the readings can be corrected for gaseous nitrogen through a flowmeter equation that is a function of geometry and density. The procedure is given in Appendix C. The calibration curve is given in Figure 10 and for the purpose of data reduction a least square curve fit was applied to the data points.

The error in mass flux comes mainly from the flow oscillations. This was generally $\pm$ 2% of full scale reading or a mass flux deviation of $\pm$ 200 lbm/hr-ft^2. As the data represents the mean of the fluctuations, the error in mass flux is less than this.

2.4 Method of Experiment

The central points in the experimental procedure were to insure that film boiling started from the entrance to the test section and that heat flux from the buss bar was controlled to the desired value, up to the point of collapse. The initial step therefore was to pass some current through

the test section to warm up before opening the liquid nitrogen supply lines. The auxiliary vacuum pump was started and run for a short while to pull down the auxiliary system to a vacuum commensurate with the pump capacity. It was observed that the test section need not be heated up to much beyond 400°F above saturation temperature before opening the liquid supply valves since with a test section initially at room temperature and a freshly delivered liquid nitrogen tank, there was sufficient heat in the supply manifold to insure that only vapor flowed into the test section for about twenty minutes from the start of the flow. The auxiliary circuit was also open to flow. During this period the wall temperature continued to rise to about 650°F above saturation temperature, sufficient to insure that film boiling was maintained when the liquid began to flow. During this initial pure vapor flow period, the air contained in the test section and any non-condensibles contained in the nitrogen tank would have been flushed out.

As the inlet manifold cooled down, an inlet thermocouple inserted inside the entrance steel tubing, fitted between the throttle valve and the test section, recorded the fluid temperature, which fell gradually to a steady value when saturated and then subcooled liquid began to flow through. The primary and secondary liquid subcoolers, fed with cooling fluid through the vacuum line, were maintained at about 5 in. Hg vacuum. The main fluid flowed through the heat exchangers at 97 psig thus insuring sufficient temperature difference to achieve liquid subcool. The subcool was obtained by reading the inlet thermocouple and the inlet pressure.

As the inlet temperature approached saturation, the test section current was increased gradually, and was brought up to 240 amperes or above depending on the flow rate, as the liquid began to flow. This corresponded to a heat flux of 12,000 BTU/hr-ft^2. The flow rate and exhaust heat exchangers were adjusted, ensuring that the pump suction gas temperature was above 50°F. The inlet pressure and liquid subcool were set to desired initial values. These changed gradually during the experiment, as the test section heat flux was lowered, but they were continually read until just before transition.

Having set the initial conditions, the system was allowed to operate until these as well as the wall temperatures assumed a steady value. Tests were run under conditions of zero heat flux from the buss bar and varying mass fluxes, two levels of constant mass flux at varying buss bar heat fluxes into the test section. An attempt was made to obtain runs for heat flux out of the test section through the buss bar, but it was discovered that the minimum temperature gradient out of the test section possible with the equipment was sufficient to progressively cool down the test section entrance until the film collapsed without the test section heat flux being altered. The stability of these tests were too poor to allow for reliable readings.

At each set of conditions, the heat flux into the test section was reduced in steps until collapse occurred. At high heat flux levels, further away from collapse, the reduction was in steps of 1.6 ampere, reducing to 0.8 amp and 0.4 amp as the collapse point was approached. At each step, the

system was allowed to run for 6 minutes or more to stabilize before the next reduction was effected. The heat flux from the buss bar was controlled by adjusting the liquid nitrogen supply rate through the heat exchanger and the current supplied to its heater. At each steady state, values of test section current and voltage, flow rate and exhaust temperatures were taken, and the buss bar temperature profile as well as the test section manometers were recorded just prior to collapse. To indicate zero heat flux into the test section from the buss bar, the last two thermocouples on the buss bar, radially spaced from the test section 1/4 inch apart and 1/4 inch from the test section outside surface, were set to indicate the same readings.

The onset of collapse, for the case of zero heat flux into the test section, was taken to be the last heat flux level prior to No. 1 thermocouple (3/4 inch from entrance) starting to experience a very rapid change in temperature with time, tracing out the typical transient profiles shown in Figures 11a and 11b. For the case of heat input into the test section the heat flux was lowered until a thermocouple (not necessarily No. 1 thermocouple) began to show the same trend. After transition had occurred the heat flux level and the setting for every other controllable parameter were left as they were at collapse, and the collapse was allowed to propagate over the test section.

2.5 Important Observations

At a given mass flux setting and initial heat flux level, it is important to note that a finite reduction in the heat flux, sometimes considerable even with zero buss bar heat input, had to be made before collapse occurred.

Moreover, after collapse had occurred, no further reduction in heat flux was necessary to allow the interface to propagate itself over the test section. The propagation was usually arrested by turning off the flow before the entire tube was wetted.

When collapse occurred with zero heat flux, the first thermocouple to be observed to indicate wetting was always No. 1 thermocouple, indicating that collapse started from the tube entrance and propagated downstream. With heat input into the test section from the buss bar, including the smallest value of buss bar heating tested, transition always occurred at about 3.5 inches from the entrance. For all the buss bar heat flux levels tested, the first thermocouple to indicate collapse was always No. 4, indicating that the region of influence of buss bar heat input approached a limit asymptotically.

In the case of heat imput into the test section from the buss bar, the liquid/vapor/solid interface which can be identified as corresponding to the burnout point, propagated itself more rapidly downstream than upstream. Buss bar heat addition was sufficient to arrest the advance of the interface upstream at least 3/4 inch from the entrance, keeping No. 1 thermocouple consistently in film boiling.

At low inlet pressures below 5 psig, rapid evaporation rate and increased test section pressure gradient helped to amplify oscillations in the flow. It was necessary therefore to throttle the exhaust flow, raising the test section pressure level and minimizing the oscillations. The primary effect of the oscillations observed in the flow meter ($\pm$ 2%) was to reduce the accuracy of the flow rate readings. It was not expected to affect the mechanism of

collapse very seriously. Very close to transition, particularly with buss bar heat flow into the test section, the intermittent evaporation, corresponding to the times when liquid wave crests washed the wall, gave rise to oscillations in flow which in a few cases caused transition prematurely than expected, by a heat flux difference of about 500 BTU/hr-ft^2.

The effect of changes in inlet pressure on the wall temperatures was very significant. It was observed that an increase in pressure of 2 psi was capable of lowering the wall temperatures by a value of the order of 30°F. A fall in pressure caused a more gradual migration of wall temperatures to higher values. At the operating pressures, 2 psi change was equivalent to a change in saturation temperature of approximately 2°F , and a change in subcool (increase for increasing pressure) slightly less than that value. The pressure effect gave rise to a combined effect of change in subcool and in the thermophysical properties of the fluid, but more particularly to the change in subcool since the percentage change in properties corresponding to a 2 psi change would be very small.

Though with high mass flux runs, the wall temperatures within the dispersed flow region, before collapse, were lower than at some upstream region within annular film boiling, collapse always originated as described earlier and propagated downstream and upstream.

Very close to collapse with buss bar heating, No. 4 thermocouple, initially at a higher level of temperatures than No. 5 and higher numbers, due to the effect of buss bar heating, would start to experience the effect of the falling film thickness more strongly than others and be reduced to a lower level of temperature.

The transient temperature profile at each station, over the collapse period (Figure 11), experienced an initial minimum in $\frac{\partial T}{\partial t}$, an inflection point, and a second minimum in $\frac{\partial T}{\partial t}$. For the case in which transition coincidentally occurred by impulse cooling at a given thermocouple station, the first minimum was taken to be equivalent to the onset of transition, Te_2 corresponding to the minimum heat flux. For the case in which such a minimum was due to the propagation of the burn-out point, the point was not particularly unique for each thermocouple for any given run. It depended on the initial temperature level before the advancing liquid interface came close to it. It could not therefore be given a unique interpretation. For the case of collapse at the entrance, the first minimum of No. 1 thermocouple would correspond to a value slightly higher than the burn-out temperature. The inflection point during propagation was observed to be unique at stations removed from the entrance. This point corresponded to the burn-out temperature.

CHAPTER III

THE TRANSITION PROCESSES

3.1 Transition Model

It was observed that for zero or finite heat into the test section from the buss bar, a finite reduction in test section heat flux, starting from a given initial state of stable film boiling, was necessary before collapse occurred. It is conventionally assumed that the film thickness profile starts from zero thickness at the transition point, increasing with distance with the liquid/vapor interface structured in a wavy form. The assumption has experimental verification. It is also assumed that the film thickness profile has a finite positive gradient at the transition point and that liquid exists on the uniformly heated surface while annular film boiling is maintained. (See for example [3]).

If this were to be the case, the wall temperature at an infinitesimal distance away from the wetting point will be infinitesimally higher than T_{wet}. Therefore a correspondingly infinitesimal decrease in test section heat flux would be required to reduce the temperature to T_{wet}, thereby permitting the interface to propagate at least up to that point. The problem is therefore not a question of collapse of film boiling but extension of nucleate boiling and rate of propagation of the burn-out interface over the rest of the tube. The model cannot therefore explain the observation stated in the first sentence of this chapter as well as the fact that once collapse had occurred no further decrease of heat flux was necessary to allow nucleate boiling to extend over the rest of the test section, with uniform heating.

It is presented here that the start of the liquid/vapor film interface in annular film boiling, at a condition of constant test section heat flux and temperatures above collapse point, does not exist on the uniformly heated test section itself but on the unheated endpiece supporting the test section (Figure 12). Moreover, the initial slope is not necessarily positive, particularly if there is radial heat addition from a buss bar or support member. For the latter case the film thickness, except for the singular point at the origin, decreases to a minimum at some distance further removed into the test section.

Two models are necessary to describe the possible modes of collapse with annular film boiling starting from the entrance, if the possibility of collapse by dispersed rewet is excluded.

3.1.1 Collapse originating from entrance of test section

This mode of collapse is axial conduction controlled and will occur in the cases of heat conduction out of the test section via an end piece or a buss bar, or for zero heat flux into the test section from the buss bar. The heating along the flow channel is discontinuous at the entrance and hence the temperature profile, and this discontinuity is particularly sharp if the end piece is an electrical and thermal insulator. This discontinuity in the temperature profile is necessary in order to start annular film boiling at the entrance, and a discontinuity in the heat flux distribution is necessary to maintain the film boiling. The shape of the liquid/vapor interface will depend on the evaporation rate, system pressure, surface tension, and velocity profile at the wall.

The temperature gradient on the unheated end piece as the point of discontinuity is approached is very high (Figure 13a). Thus it is possible for the wall temperature only a small distance upstream of the point to be equal to the wetting temperature and allow contact of liquid and boundary. For a given decrease in heat flux, the migration distance of the wetting point, on account of this high temperature gradient, will be of a much smaller order of magnitude, with the result that it will take a sizeable decrease in heat flux to permit the wetting interface to migrate to the test section. The migration is controlled chiefly by axial conduction. The wetting interface is sufficiently near the end of the test section that temperature equilibrium between it and the test section end will be immediately achieved as soon as conditions allow. Thus wetting of the test section, and hence transition, will occur as soon as the heat flux is lowered to such a level that the combined effect of heat transfer through the film into the liquid, axial conduction from the test section into the end piece, and intermittent cooling by the oscillating advancing liquid/wall contact point, of the test section end, permit the test section end to attain the wetting temperature.

A mathematical model for the solution of the above situation is given below (see Figure 13b).

Energy equation for the insulator (wall temperature = T').

$$\frac{\partial^2 T'}{\partial x^2} + \frac{1}{r}\frac{\partial}{\partial r}\left(r\frac{\partial T'}{\partial r}\right) = \frac{1}{\alpha}\frac{\partial T'}{\partial t} \qquad (17)$$

Boundary Conditions

$$k_1\left(\frac{\partial T'}{\partial r}\right)_{r=0} + h_1 (T_w' - T_i) = 0 \tag{18}$$

$$\left(\frac{\partial T'}{\partial r}\right)_{r=\eta_1} = 0 \tag{19}$$

$$\left(\frac{\partial T'}{\partial x}\right) = 0 \qquad \eta_2 < r \leq \eta_1 \tag{20}$$

$$k_1\left(\frac{\partial T'}{\partial x}\right)_{x=0} = -k_2\left(\frac{\partial T''}{\partial z}\right)_{z=0} \qquad 0 \leq r \leq \eta_2 \tag{21}$$

$$T'(0, r, t) = T''(0, r, t) \qquad 0 \leq r \leq \eta_2 \tag{22}$$

$$T_w'(\infty, r, t) = T_1' \tag{23}$$

$$T_w'(x, 0, 0) \quad \text{given} \tag{24}$$

Test Section

The tube may be treated as a thin flat plate of thickness

$$k_2\left(\frac{\partial^2 T''}{\partial z^2}\right) + k_2\left(\frac{\partial^2 T''}{\partial r^2}\right) + q = \rho_2 c_2 \frac{\partial T''}{\partial t} \tag{25}$$

$$k_2\left(\frac{\partial T''}{\partial r}\right)_{r=0} + h_2 (T_w'' - T_i) = 0 \tag{26}$$

$$-k_1\left(\frac{\partial T'}{\partial x}\right)_{x=0} = k_2\left(\frac{\partial T''}{\partial z}\right)_{z=0} \qquad 0 \leq r \leq \eta_2 \tag{27}$$

$$-k_2\left(\frac{\partial T''}{\partial r}\right)_{r=\eta_2} = q_2 \qquad 0 \leq z \leq a \tag{28}$$

$$\left(\frac{\partial T''}{\partial r}\right)_{r=\eta_2} = 0 \qquad x > a \tag{29}$$

$$T_w'(0, r, t) = T_w''(0, r, t) \tag{30}$$

$$T_w(z, 0, 0) \quad \text{GIVEN} \tag{31}$$

h_1 may be taken as approximately equal to forced convection heat transfer coefficient. h_2 may be approximately given by a laminar analysis of the vapor film layer since the film may be considered to be in laminar flow within a short distance of the entrance.

An approximate analytic solution of the above problem will be very difficult on account of the discontinuous boundary conditions. A numerical solution will be more appropriate. Work on the subject of this thesis is still in progress, and the results of such a solution is expected to be one of the final outputs.

3.1.2 Impulse cooling collapse

For the case of radial heat input from a buss bar or end connection, collapse at the entrance is prevented. The mechanism of collapse is deemed to be as given by Kalinin et al. [2] and presented earlier. The occurrence of hydrodynamic instability of the liquid/vapor interface is no guarantee that transition to nucleate boiling will occur. When the liquid hits the wall after such an instability, the wall temperature may be still too high to sustain liquid contact.

The heat transfer on impact of a wave is controlled not only by conduction through the liquid but also by a probable turbulent diffusivity of the liquid, at least during the initial period of contact. However, it would be a justifiable approximation to ignore the turbulent contribution, though a more appropriate approximation would be to replace the laminar diffusivity of heat by a sum of the laminar and eddy diffusivities of heat. Starting from a given set of initial conditions, before the first wave hits the wall, the effect of repeated waves hitting the wall until collapse occurred

can only be completely solved if the impact duration, the wall temperature recovery factor between waves, and the wave distribution are known.

3.1.2.1 Effect of heat flux

Reference [2] treated the case of a quenched tube with no heat addition. For a heated test section the start of collapse would occur at a lower wall temperature since the heat addition would reduce the contact time of each wave crest, reduce the wall temperature decrease at each impulse cooling, and increase the overall contact period from first contact to collapse. It was thought probable that for a test section at a given initial temperature the heat generated and transferred during the contact period could be a negligible proportion of the heat that would be transferred during an impulse quenching process from the same initial temperature. This would make eq. (10) and (11) applicable for a given pair of highly wetting liquid and tube material. To correlate with these equations would give just one point on the curve since the tests in this thesis were for a single liquid/tube combination.

Choosing a typical initial wall temperature of $420°R$, liquid subcool of $7°R$, system pressure of 21 psia, eq. (7), (8), and (9) were solved graphically for the heat-up time t.

Heat transferred by quenching during this time is given by

$$Q_q = -k\int_0^{t^\circ}\left(\frac{\partial T}{\partial r}\right)_{r=0} dt \approx \frac{2}{\sqrt{\pi}}(T_{cb}-T_{Lo})\sqrt{(k\rho c)_L t^\circ} \qquad (32)$$

The results of the solution are given in Appendix B. With a typical heat flux at collapse of 4,500 BTU/hr-ft^2 , the ratio of resistance heating flux to quenching flux was approximately 20%. This would indicate a negligible effect of test section resistance heating at collapse. A modified conduction model solution indicated an additive effect of test section heating to that of a quenched wall, on the collapse temperature. The additive term, however, was a function of an undetermined contact time.

CHAPTER IV

RESULTS AND DISCUSSION

As the collapse interface propagates downstream and upstream of the tube, depending on the position at which collapse originated, each thermocouple traces out a transient profile as indicated in Figure 11. The point of minimum slope at the higher temperature level corresponds to point of minimum heat flux in the boiling curve and the point of inflection corresponds to the burn-out point.

Figures 14a, b, c, and d are plots of wall temperature profiles shortly before collapse for the first 15 inches from the entrance. The lowest temperature points indicate the regions of eventual collapse from which nucleate boiling would spread to the rest of the test section. Figures 14a, b, and c are for heat addition from the buss bar into the test section, at various (q/A)BB levels and various mass fluxes. The first thermocouple position to collapse for these runs and for other runs with heat flux into the test section was No. 4, located 3.5 inches from the entrance, and the temperature profiles clearly indicate this. A change of buss bar heat flux from 36,600 BTU/hr-ft^2 (Figure 14a) to 107,400 BTU/hr-ft^2 (Figure 14b) only moves the collapse point by less than 0.5 inches into the test section. Figure 14d is for zero buss bar heat flux and the collapse originated from the test section entrance.

It was observed that the collapse interface advanced at constant speed at least for some initial period. Figures 15a, b, c, and d are plots of the time at which each thermocouple transient profile indicates an inflection

point, vs. the position of the thermocouple, and these graphs correspond in that order to the runs of Figure 14. After an accelerating period, the propagation rate definitely attains a constant value. Comparing Figures 10 and 11, it would appear that the velocity will remain constant at a value determined by the mass flux, test section heat flux, and initial level of wall temperatures over approximately constant wall temperatures just before collapse. In the theory of the spread and resorption of a calefaction spot on a heated wall, Semeria and Martinet [8] assumed that the wall/liquid/vapor interface would advance at a constant temperature. According to the above observation, the assumption is expected to hold if the initial wall temperatures were constant over the film boiling region slightly removed from the interface.

Figures 16a and b are plots of minimum heat flux just prior to collapse vs. the buss bar heat flux into the test section, and at mass flux levels of 62,500 lbm/hr-ft^2 and 98,000 lbm/hr-ft^2 . At zero buss bar heat flux, the wetting interface prior to collapse is at the unheated insulating piece at the end of the test section but close to the heated tube at some equilibrium temperature. As a result of this proximity, the wall temperature at the entrance is kept as close as possible to the liquid temperature, due to axial end conduction, and the liquid is immediately available to wet the surface as soon as the heating condition allows. Moreover, the film temperature profile is at a minimum at the entrance and hence the wall temperature is at a minimum there.

With radial heat flux into the test section from the buss bar, the effect of the buss bar is maximum at the entrance, where the boiling rate and the film thickness are higher than, for example, 3.5 inches downstream. Figures 15a, b, and c indicate the resulting temperature profile, Collapse point is shifted downstream and a different collapse mechanism, as explained earlier, becomes effective. The experimental evidence indicates that the resulting minimum heat flux at collapse is lower than for collapse originating at the end. Moreover, at a buss bar heat flux close to or greater than 40,000 BTU/hr-ft^2 , the collapse heat flux is unaffected by buss bar heating, and for a given mass flux occurs at a constant heat flux.

Within the asymptotic regions of the plots of collapse test section heat flux vs. buss bar heat flux, Figure 16 does not show a mass flux effect. Figure 17, however, shows the slight but definite effect of mass flux at a constant buss bar heat flux of 41,000 BTU/hr-ft^2. At increased mass flux, the heat transfer coefficient of the vapor film prior to collapse is higher. Hence, wall temperatures are lower for the same heat flux and closer to the collapse value. Moreover, as the wave crests sweep along the tube surface at a higher velocity, the heat transfer coefficient is higher and the wall temperatures lowered by a higher amount at each impulse. Thus it is to be expected that the temperature conditions for collapse will be satisfied at a higher heat flux with a higher mass flux. Hence the observed increase in collapse heat flux with mass flux. Figure 18 is a similar plot but with varying buss bar heat fluxes greater than or close to 40,000 BTU/hr-ft^2. At a given mass flux, the collapse heat flux is within 5% of the value given by Figure 17, at the worst deviation, indicating the degree of repeatability

of the results, since within this range of buss bar heat flux, the buss bar heating is not expected to influence the collapse.

The explanation given above for the observed increase in collapse heat flux with mass flux tacitly implies that the satisfaction of the temperature condition for collapse is more critical than for the heat flux. Figure 19 supports this argument. For a constant (q/A)BB > 41,000 BTU/hr-ft^2, $(T_w - T_s)$ at collapse was constant within experimental errors at a value of 244°R . A plot of $(T_w - T_s)$ at collapse vs. mass flux, for (q/A)BB greater than 40,000 BTU/hr-ft^2 is shown in Figure 20. The points are within scatter of $\pm$ 10% about a mean constant value of 228°R.

As a result of this, a calculation for the collapse temperature in pool boiling using Berenson's expression [5]

$$\Delta T_{min} = \frac{0.127 \rho_{vf} h_{fg}}{k_{vf}} \left[\frac{g(\rho_l - \rho_v)}{(\rho_l + \rho_v)}\right]^{2/3} \left[\frac{g_o \sigma}{g(\rho_l - \rho_v)}\right]^{1/2} \left[\frac{\mu_f}{g(\rho_l - \rho_v)}\right]^{1/3} \quad (33)$$

was made at a film temperature of 180°R and a pressure of 1 atmosphere. They predicted ΔT_{min} was 243°R . The measured value of 228°R from Figure 20 is within 6% of the prediction. Heat flux calculated with the corresponding minimum pool boiling heat flux correlation was lower than the measured value as expected (Figure 23).

It may be concluded that within the range of mass fluxes tested, the film boiling collapse temperature is independent of mass flux and is correlated within 6% by the pool boiling correlation of Berenson [5]. The collapse heat flux is, however, dependent on mass flux.

Figures 21a and 21b are plots of $(T_w - T_s)$ vs. $(q/A)BB$ at collapse, and at constant mass fluxes. A similar effect of buss bar heat flux is observed, as for the effect on collapse heat flux.

Figure 22 shows the effect of mass flux on collapse heat flux at zero buss bar heat input. The expected trend is indicated but the data scatter is very high, indicating the difficulty of controlling buss bar heat input to a zero value.

4.1 Conclusion

(a) Collapse mechanism of annular film boiling to nucleate boiling is either axial conduction controlled or impulse cooling controlled.

(b) Axial conduction controlled collapse occurs at the entrance to the test section of a uniformly heated wall. The discontinuity in the heating and temperature profiles, starting from the entrance, are necessary to start and maintain the film boiling.

(c) Impulse cooling controlled collapse occurs downstream of the test section, with heat addition from an upstream buss bar. Within this region, the collapse heat flux and temperatures are unaffected by buss bar heating.

(d) Once collapse occurred, no further reduction in heat flux was necessary to cause the collapsed interface to propagate through the test section.

(e) The propagation velocity, starting from collapse, builds up to a constant value as long as the wall temperatures across which the interface propagates, were fairly at a uniform value just prior to collapse.

(f) Hydrodynamic instability of the vapor/liquid interface may occur, permitting the liquid to hit the wall. However, the wall temperature may be so high that rapid evaporation occurs, forcing the interface off the heated surface. It may of course be low enough to sustain liquid contact. This leads to the conclusion that hydrodynamic instability is no guarantee of collapse in film boiling, but is not an excluded criterion.

(g) The collapse heat flux was a function of mass flux, but the collapse temperature difference $(T_w - T_s)$ was independent of mass flux. This led to two conclusions. First, that the collapse condition is more likely to be thermodynamically determined, i.e. the wall temperature must be low enough to permit liquid/solid contact. Second, that the collapse temperature difference $(T_w - T_s)$ could possibly be predicted by the pool boiling correlation. Using Berenson's expression [5], the calculated value was $243°R$, and the average experimental value was $228°R$, giving an error of 6% which is quite satisfactory.

(h) There are three as yet inconclusive propositions now existing in the literature for the calculation of ΔT_{min} :

(a) $\frac{T_w}{T_c} = .84 \qquad \left(\frac{P}{P_c} < 10^{-3}\right)$ (Spiegler et al. [9])

(b) $\frac{\Delta T_{min}}{T_c - T_l} = 0.165 + 2.48\left[\frac{(k\rho c)_l}{(k\rho c)_w}\right]^{1/4}$ (Kalinin [2])

(c) Berenson's pool boiling ΔT_{min} (this report)

All these apply to forced flow impulse cooling collapse of subcooled or very low quality liquid.

4.2 Suggestions for Future Research

Work on the subject of this thesis is still in progress. The main areas of future concentration are:

(i) The formulation of a criterion for impulse cooling collapse and the solution of the resulting model.

(ii) The solution of the problem for end conduction controlled collapse.

(iii) Extension of the research to saturated and quality inlet.

(iv) Effects of twisted tape and of wall surface material on collapse. Test sections with bends in the flow direction should also be considered.

(v) It would also be very informative to obtain a visual evidence of the predominance of thermodynamical instability in controlling collapse. This may be obtained by observing for the occurrence of repeated hitting of the boiling surface by the liquid, and its re-evaporation without causing collapse.

(vi) The equipment is much too bulky for some very finely controlled experiments that need to be made. The buss bar heat flux control needs to be changed so as to be able to maintain stable conditions under heat flow out of the test section from the buss bar.

REFERENCES

1. S. J. Hynek, W. M. Rohsenow, and A. E. Bergles, "Forced Convection Dispersed Flow Boiling," Report No. DSR 70586-63, Department of Mechanical Engineering, MIT, 1969.

2. E. K. Kalinin et al., "Investigation of the Crisis of Film Boiling in Channels," Moscow Aviation Institute, USSR, 1968.

3. F. F. Simon and R. J. Simoneau,"Transition from Film to nucleate Boiling in Vertical Forced Flow," NASA TMX-52597, 1967.

4. R. S. Dougall, W. M. Rohsenow, "Film Boiling on the Inside of Vertical Tubes with Upward Flow of Fluid at Low Qualities, MIT Report No. 9079-26, 1963.

5. P. Berenson, "Transition Boiling Heat Transfer From Horizontal Surfaces," Ph.D. Thesis, Dept. of Mechanical Engineering, MIT, 1960.

6. L. A. Bromley, "Heat Transfer in Stable Film Boiling," Chem. Eng. Prog., 46, 221-227, 1950.

7. A. E. Coury and A. E. Dukler, "Turbulent Film Boiling on Vertical Surfaces: A Study Including the Influence of Interfacial Waves," University of Houston, Houston, Texas.

8. R. Semeria and B. Martinet, "Calefaction Spots on a Heated Wall, Temperature Distribution and Resorption," presented at IME Symposium on Boiling Heat Transfer in Steam Generating Units and Heat Exchangers, Manchester, England, September 15-16, 1965.

9. P. Spiegler et al., "Onset of Stable Film Boiling and the Foam Limit," Int. J. Heat and Mass Transfer, Vol. 6, 1963.

10. H. Merte and J. A. Clark, "Boiling Heat Transfer with Cryogenic Fluids at Standard, Fractional, and Near-Zero Gravity," J. of Heat and Mass Transfer, Vol. 86, No. 3, 1964.

11. E. K. Kalinin et al., "Heat Transfer in Tubes with Rod Regime in the Case of Film Boiling of Subcooled Liquids," Moscow Aircraft Institute, USSR. (Cocurrent Gas-Fluid Flow, Plenum Press, 1969.).

12. R. K. F. Keeys et al., "Post Burnout Heat Transfer in High Presuure Steam Water Mixtures in a Tube with Cosine Heat Flux Distribution," United Kingdom Atomic Energy Authority, Report No. AERE-R 6411, 1971.

13. R. P. Forslund, W. M. Rohsenow, "Thermal Non-Equilibrium in Dispersed Flow Film Boiling in a Vertical Tube," MIT Report No. 75312-44, Department of Mechanical Engineering, MIT, 1966.

14. T. G. Beckwith and N. L. Buck, Mechanical Measurements, Addison-Wesley Publishing Co., Reading, Massachusetts, 1961.

APPENDIX A

DERIVATION OF TEMPERATURE DIFFERENCE ACROSS TUBE WALL

Let W be the geat generation per unit volume of the tube. Let U be the thermal resistance of the insulation around the test section in $(BTU/hr\text{-}ft^2{}^\circ F)^{-1}$. Let ℓ, K, r_i, and r_o be the length, conductivity, inside and outside radii respectively of the tube. In observing the effect of a small temperature change on the physical properties of Inconel 600, it is a good assumption that the properties are constant.

With a uniform W and K, the solution to the conductance equation in cylindrical coordinates gives

$$T = -\frac{W}{4K} r^2 + C_1 \ln r + C_2 \tag{A-1}$$

with boundary conditions

$$T = T_o \quad \text{at} \quad r = r_o \tag{A-2}$$

and

$$K \frac{\partial T}{\partial r}\Big|_{r_o} = \left[\frac{T_{ambient} - T_o}{U}\right] \tag{A-3}$$

Equation (A-2) gives

$$T_o = -\frac{W}{4K} r_o^2 + C_1 \ln r_o + C_2 \tag{A-4}$$

Equation (A-3) gives for $T_{ambient} = 80°F$

$$-\frac{W}{2K} r_o + \frac{C_1}{r_o} = \left[\frac{80 - T_o}{UK}\right] \tag{A-5}$$

Equations (A-4) and (A-5) give

$$C_1 = \frac{(80 - T_o) r_o}{U K} + \frac{W}{2K} r_o^2 \qquad \text{(A-6)}$$

$$C_2 = T_o + \frac{W r_o^2}{4K} - \ln r_o \left[\frac{(80 - T_o) r_o^2}{U K} + \frac{W r_o^2}{2K} \right] \qquad \text{(A-7)}$$

Substituting (A-6) and (A-7) into (A-1) and evaluating the resulting equation at r_i gives

$$T_i = T_o + \frac{W}{4K}(r_o^2 - r_i^2) - \ln\left(\frac{r_o}{r_i}\right)\left[\frac{(80 - T_o) r_o^2}{U K} + \frac{W r_o^2}{2K} \right] \qquad \text{(A-8)}$$

The final step in the solution is the determination of U for the apparatus. This was accomplished by applying a small fraction of the normal power to the test section with no flow through the tube. When equilibrium is achieved, the wall temperature is recorded along with the power level. This was done for several power levels. Assuming all heat generated passes through the insulation gives one a means of calculating the thermal resistance using the following equation:

$$U = \frac{\Delta T}{q/A\,|_{r_o}} \qquad \text{(A-9)}$$

where

$$q/A\,|_{r_o} = \frac{W \pi \ell (r_o^2 - r_i^2)}{2 \pi \ell r_o} \qquad \text{(A-10)}$$

The data resulting from this experiment is plotted in Figure 24. As $(T_w - 80)$ at collapse is about 300°F, U is taken to be 0.95 $(\text{BTU/hr-ft}^2\text{°F})^{-1}$ for the data reduction.

APPENDIX B

EFFECT OF HEAT GENERATION IN TEST SECTION ON COLLAPSE

For the solution of eq. (8), a typical set of wall temperature, system pressure, and liquid temperature was chosen.

P_L = 21 psia = 1.43 atmospheres

T_L = 77°K

T_{sat} = 80.6°K

$T_{subcool}$ = 3.6°K

P_c = 33.54 atmospheres } Thermodynamic Critical State of Nitrogen

T_c = 126°K }

T_{wo} = 420°R ≅ 234°K

$(q/A)_{ts}$ = 4,500 BTU/hr-ft^2

$$\sqrt{\frac{(k\rho C)_L}{(k\rho C)_w}} \quad \sqrt{\frac{(0.0782 \times 49.8 \times 0.494)}{(9 \times 530 \times 0.109}} = 0.0608 \qquad \text{(B-1)}$$

$$\sqrt{\frac{(k\rho C)_w}{(k\rho C)_L}} = 16.44 \qquad \text{(B-2)}$$

$$\frac{\Delta T_{sub}}{(T_c - T_s)} = \frac{3.6}{45.4} = 0.0793 \qquad \text{(B-3)}$$

$$P/P_c = 0.0427 \qquad \text{(B-4)}$$

δ_w = 0.127 cm

α_L = 8.2 x 10^{-4} cm^2/s

α_w = 4.02×10^{-2} cm^2/s

$(T_{wo} - T_{Lo})$ = 157°K

Substituting these values into eq. (8), we have

$$T(y,t) - 77 = 148\left[\operatorname{erfc}\frac{y}{.057\sqrt{t}} - 0.115\operatorname{erfc}\left(\frac{y}{.057\sqrt{t}} + \frac{.317}{\sqrt{t}} + \ldots\right)\right] \quad \text{(B-5)}$$

The equation is plotted in Figure 25 for the following values of y :

$y = 0.05 \times 10^{-4}$ cm

0.10×10^{-4} cm

0.50×10^{-4} cm

1.00×10^{-4} cm

It is seen that the maximum temperatures occurred at $t \cong 10^{-2}$ sec. Since the order of magnitude of the contact time was what was desired, it was not necessary to solve the complete set of equations (7), (8), and (9). The contact time was taken as 10^{-2} seconds.

From eq. (32) heat transfer due to quenching in 10^{-2} seconds is 0.68 BTU/ft^2. Heat generated and transferred during this period from the test section was 0.128 BTU/ft^2 . Percentage ratio is then equal to 20% approximately.

APPENDIX C

CORRECTION OF FLOWMETER CALIBRATION FOR DENSITY CHANGE

In reference [14] there is presented a flowmeter equation in the form

$$Q = A_w C \left[\frac{2g V_f (\rho_f - \rho_w)}{A_f \rho_w} \right]^{1/2} \tag{C-1}$$

where $A_w C \left[\frac{2g V_f}{A_f} \right]^{1/2}$ is just a function of flowmeter geometry and equal to a constant called α for each particular flowmeter. This reduces eq. (C-1) to the following form:

$$Q = \alpha \left[\frac{\rho_f - \rho_w}{\rho_w} \right]^{1/2} \tag{C-2}$$

where ρ_f = density of flowmeter float

ρ_w = density of fluid to be measured

Knowing the flow rate and densities in the above relations allows the solution for α which is constant for any density fluid that is used in conjunction with the particular flowmeter.

$$\alpha_{FLOWMETER} = \frac{Q}{\left[\frac{\rho_f - \rho_w}{\rho_w} \right]^{1/2}} \tag{C-3}$$

Therefore, the correction for density change at the specific flow rate that $\alpha_{flowmeter}$ was calculated for is given as

$$Q_{\substack{ANY\ DENSITY \\ FLUID}} = \alpha_{FLOWMETER} \left[\frac{\rho_f - \rho_{FLUID}}{\rho_{FLUID}} \right]^{1/2} \tag{C-4}$$

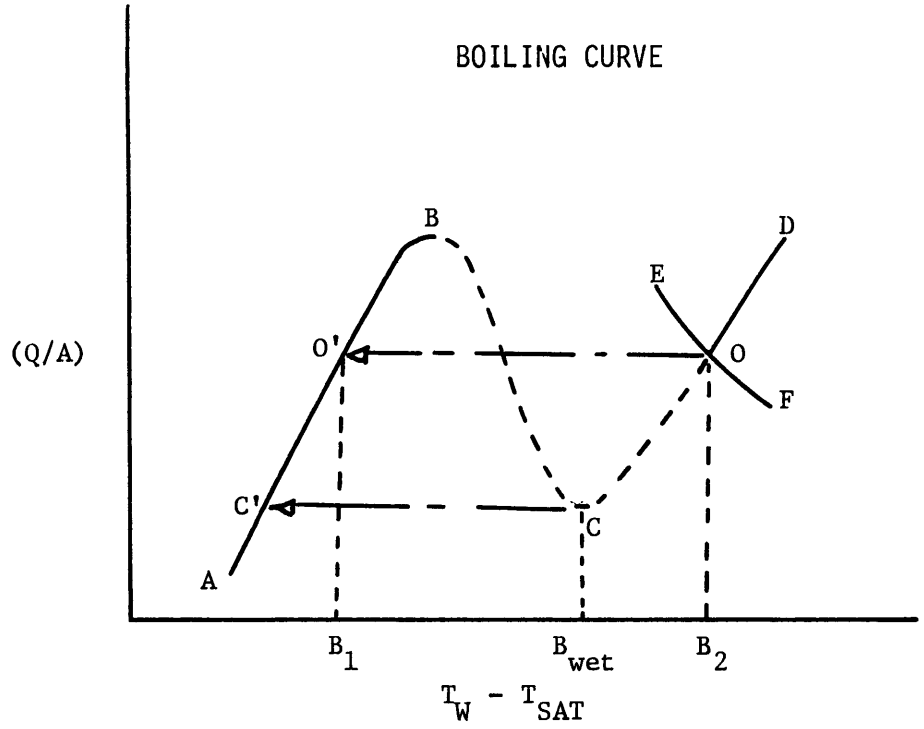

FIGURE 1

FILM BOILING VAPOR - LIQUID INTERFACE

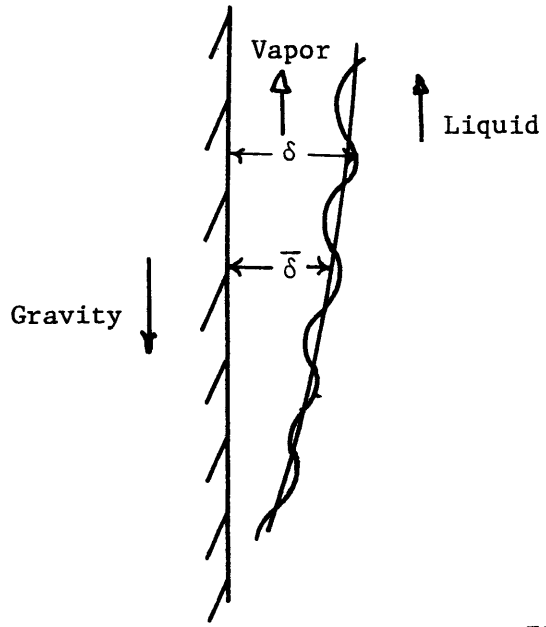

FIGURE 2

TYPE I FILM BOILING

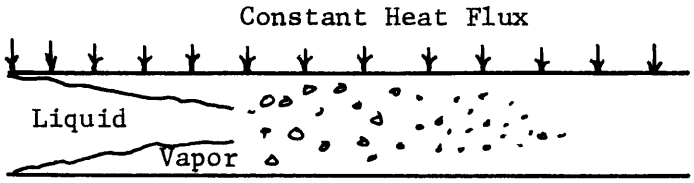

FIGURE 3a

TYPE I FILM BOILING
TEMPERATURE PROFILE

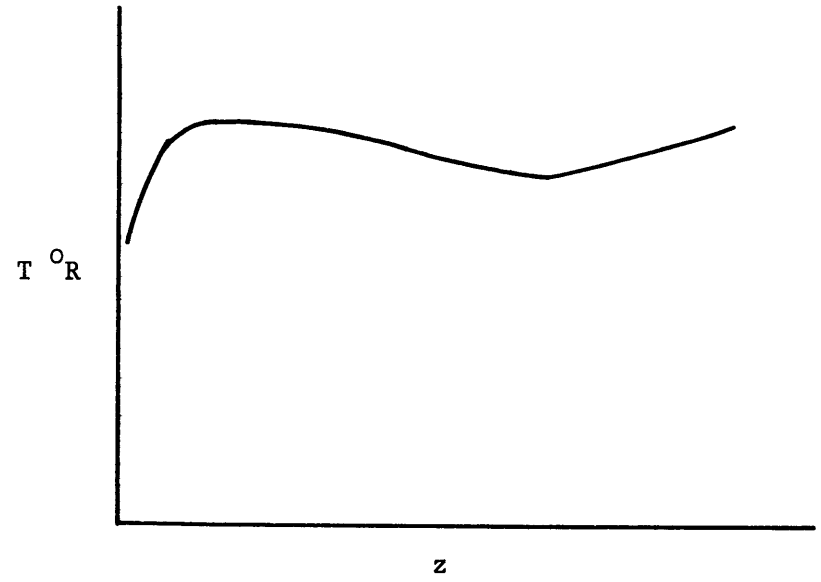

FIGURE 3b

VELOCITY PROFILE IN VAPOR FILM

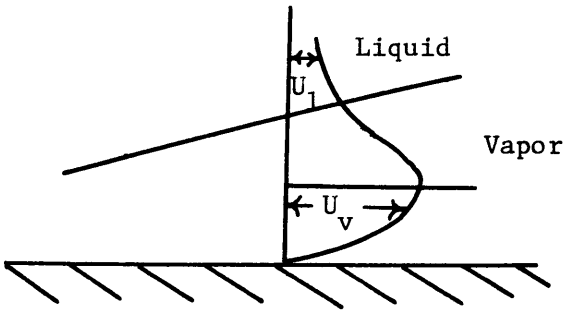

FIGURE 4

TYPE II FILM BOILING

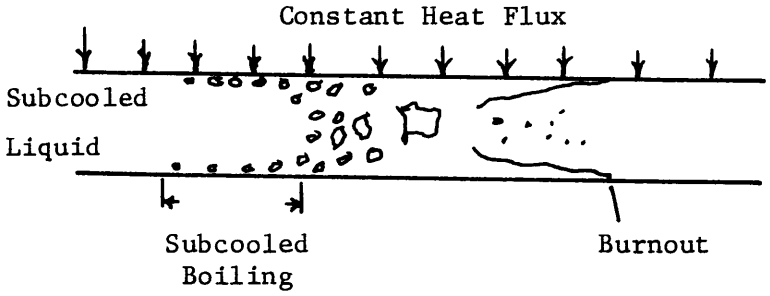

FIGURE 5a

TYPE II FILM BOILING
TEMPERATURE PROFILE

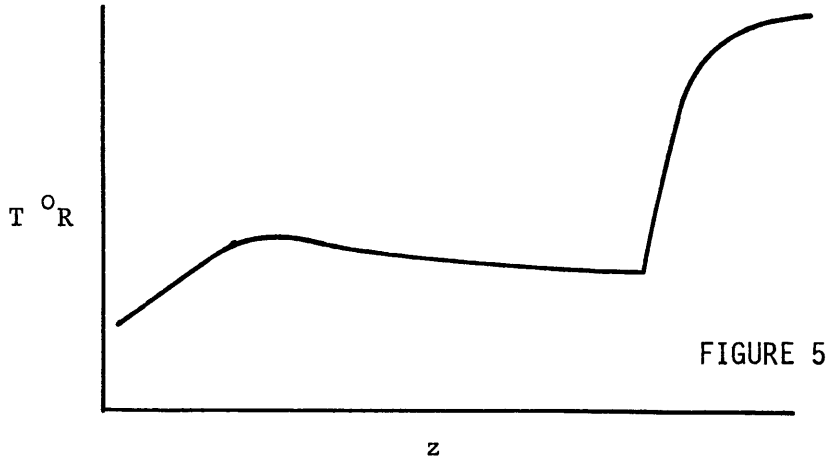

FIGURE 5b

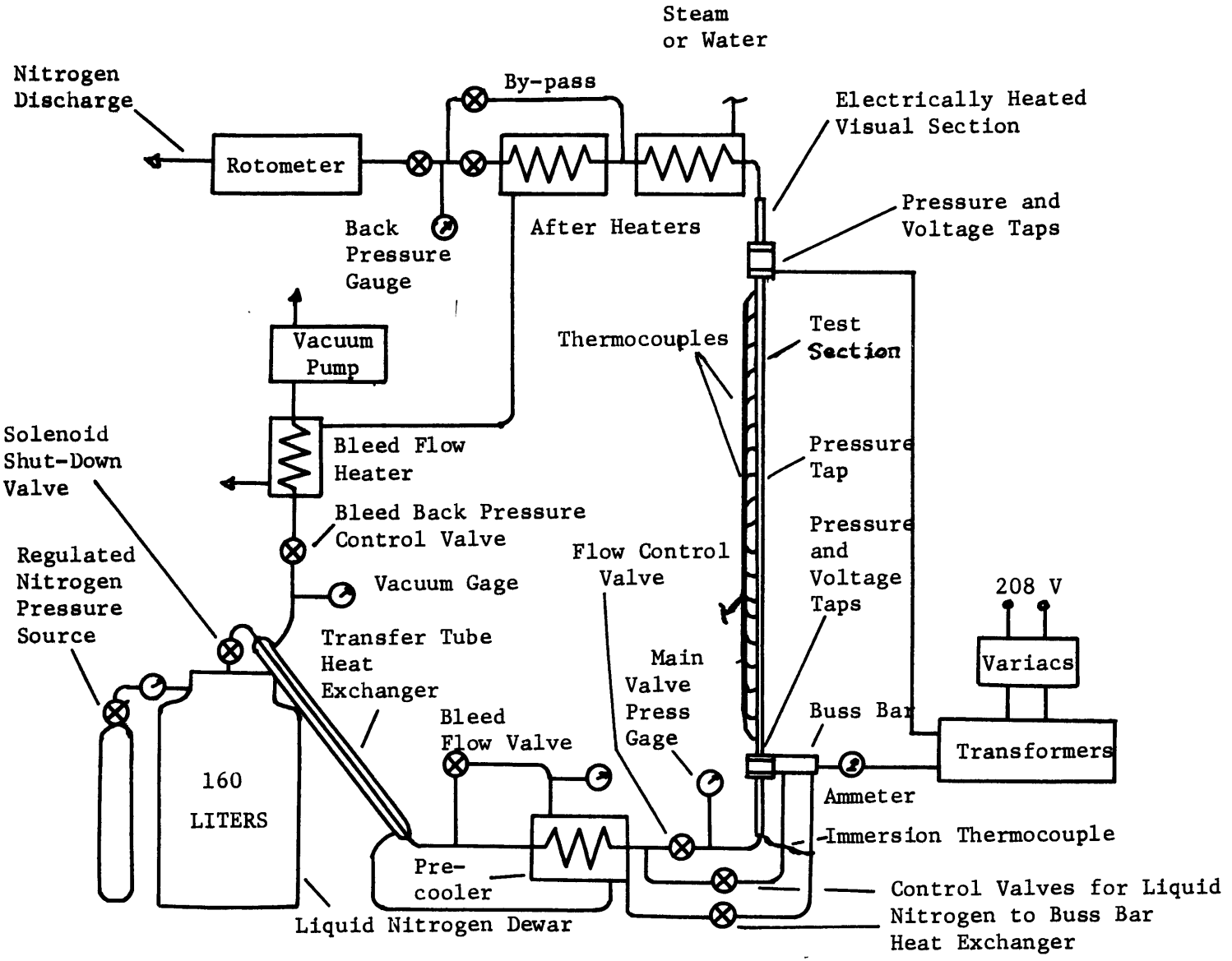

SCHEMATIC DIAGRAM OF THE TEST APPARATUS

FIGURE 6

LOW TEMPERATURE CALIBRATION OF COPPER - CONSTANTAN THERMOCOUPLE USING LIQUID NITROGEN

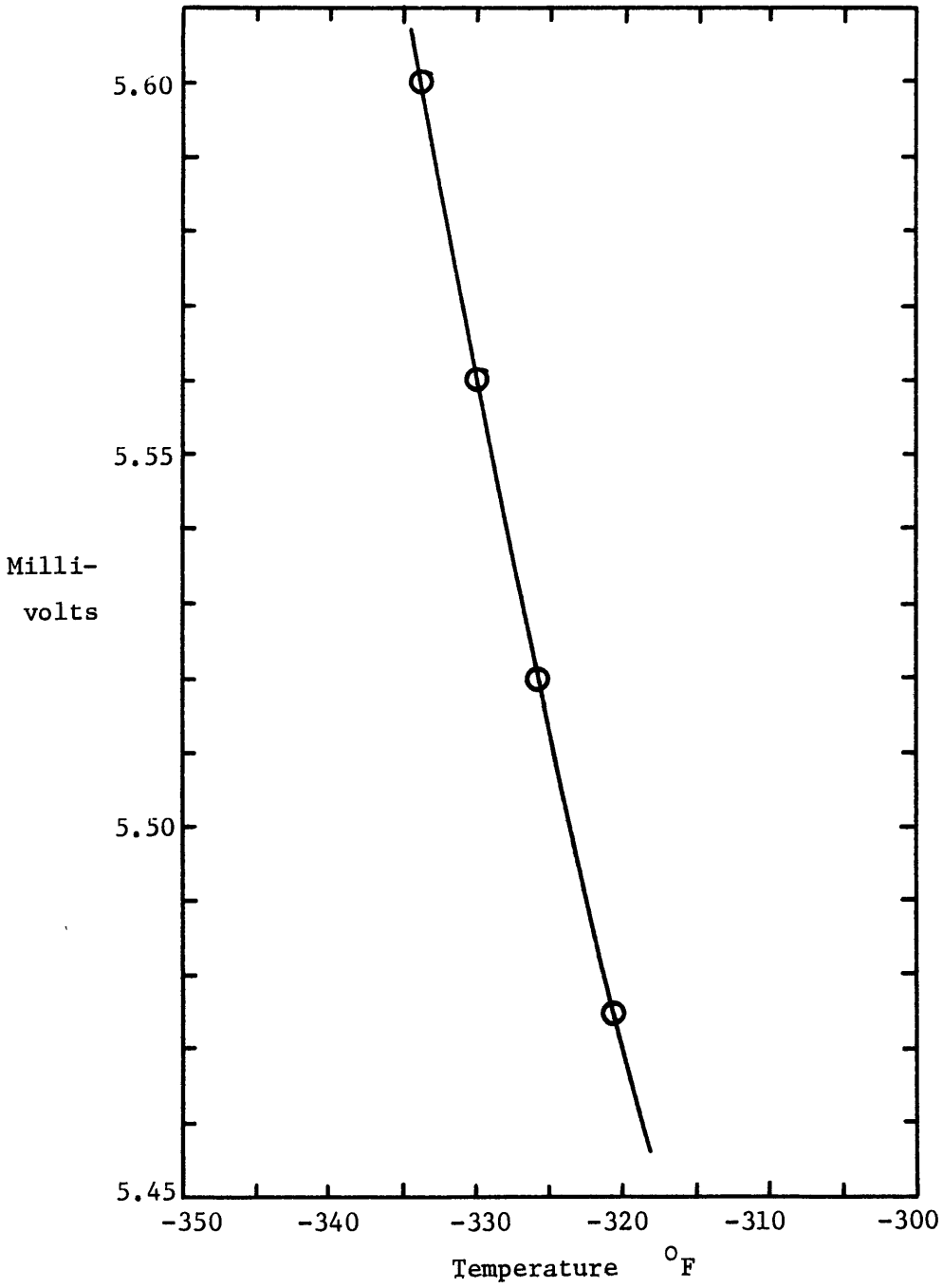

FIGURE 7

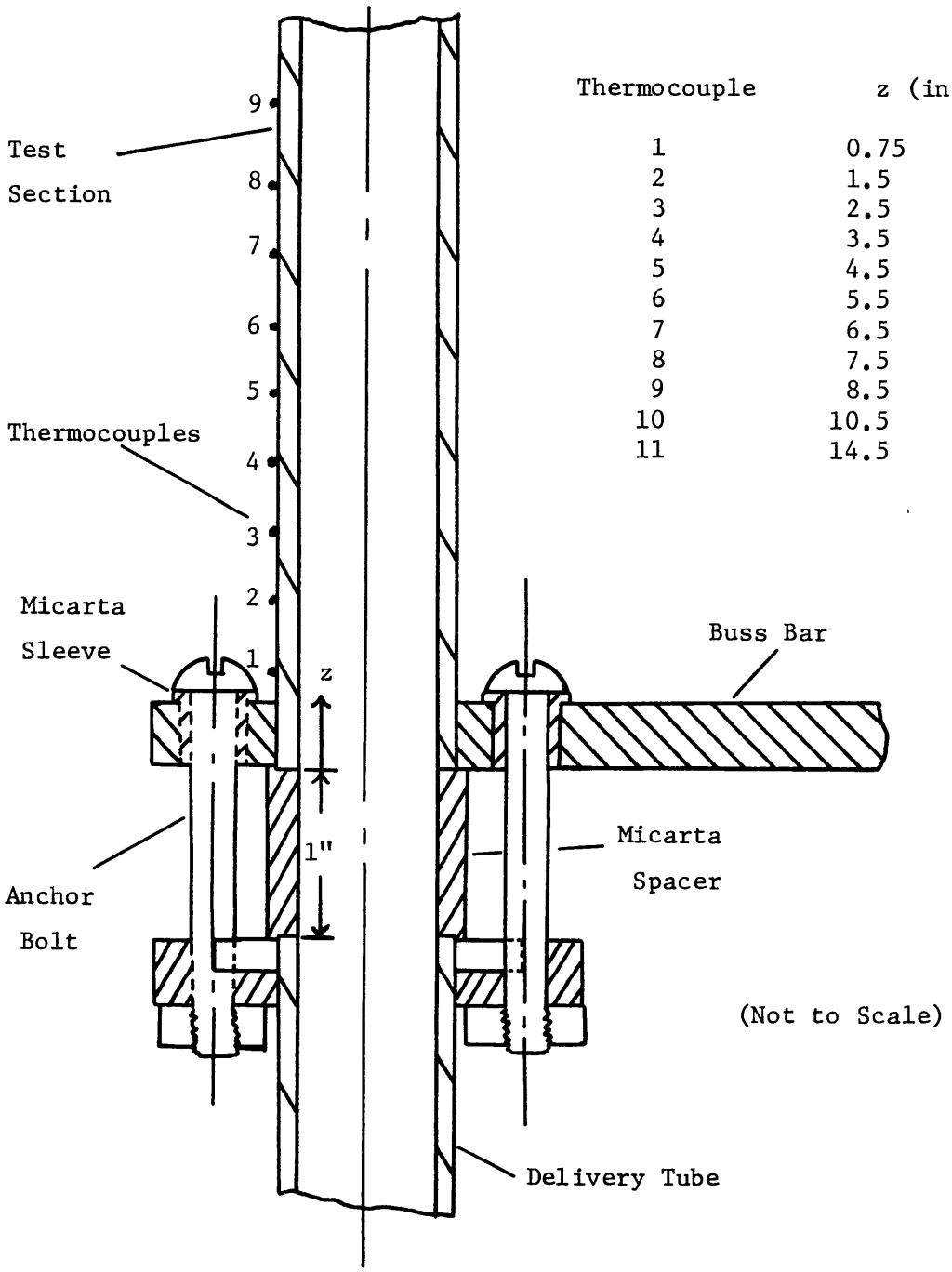

Thermocouple	z (inch)
1	0.75
2	1.5
3	2.5
4	3.5
5	4.5
6	5.5
7	6.5
8	7.5
9	8.5
10	10.5
11	14.5

TEST SECTION INLET CONFIGURATION

FIGURE 8

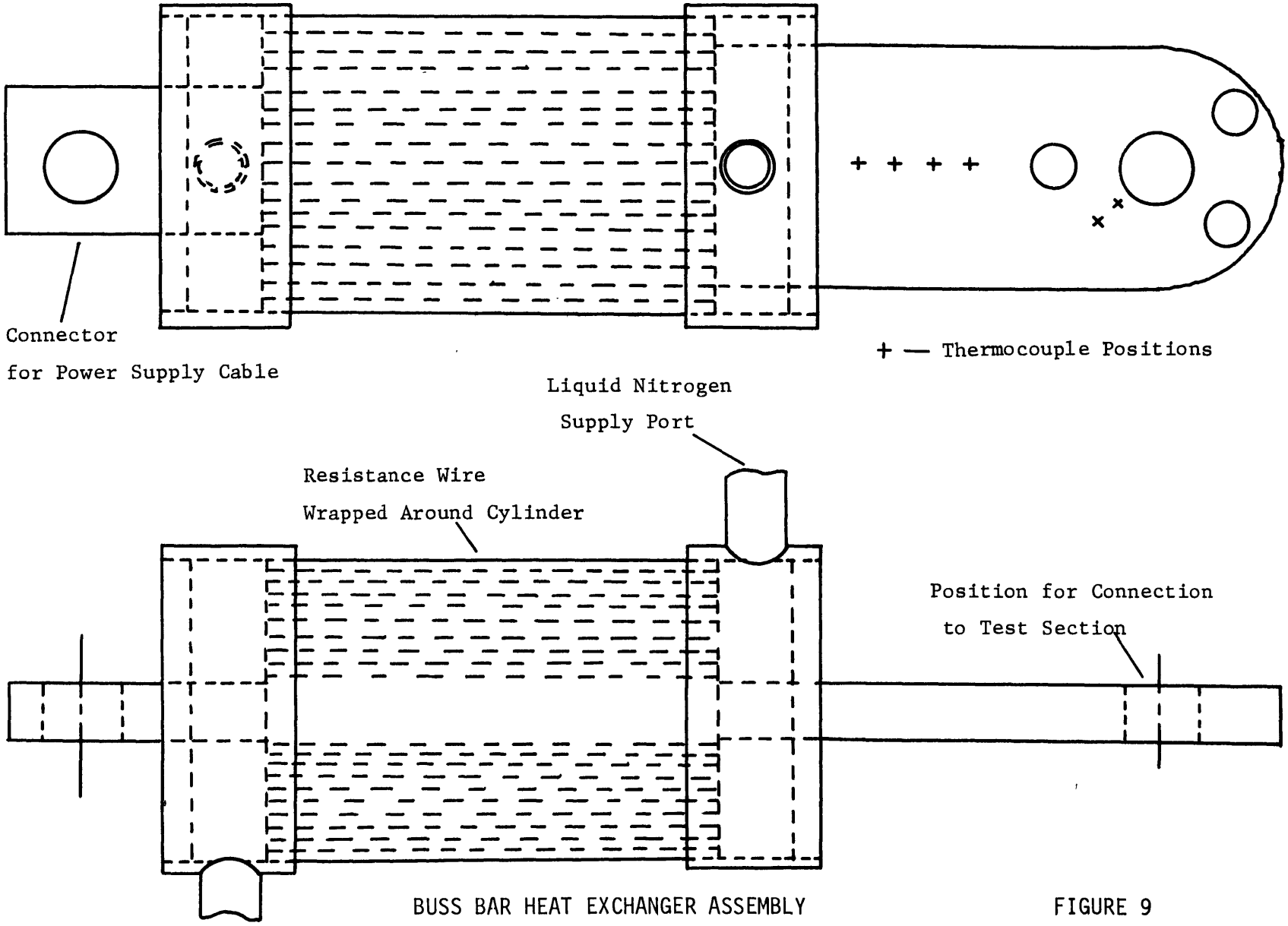

BUSS BAR HEAT EXCHANGER ASSEMBLY

FIGURE 9

FLOW METER CALIBRATION CURVES

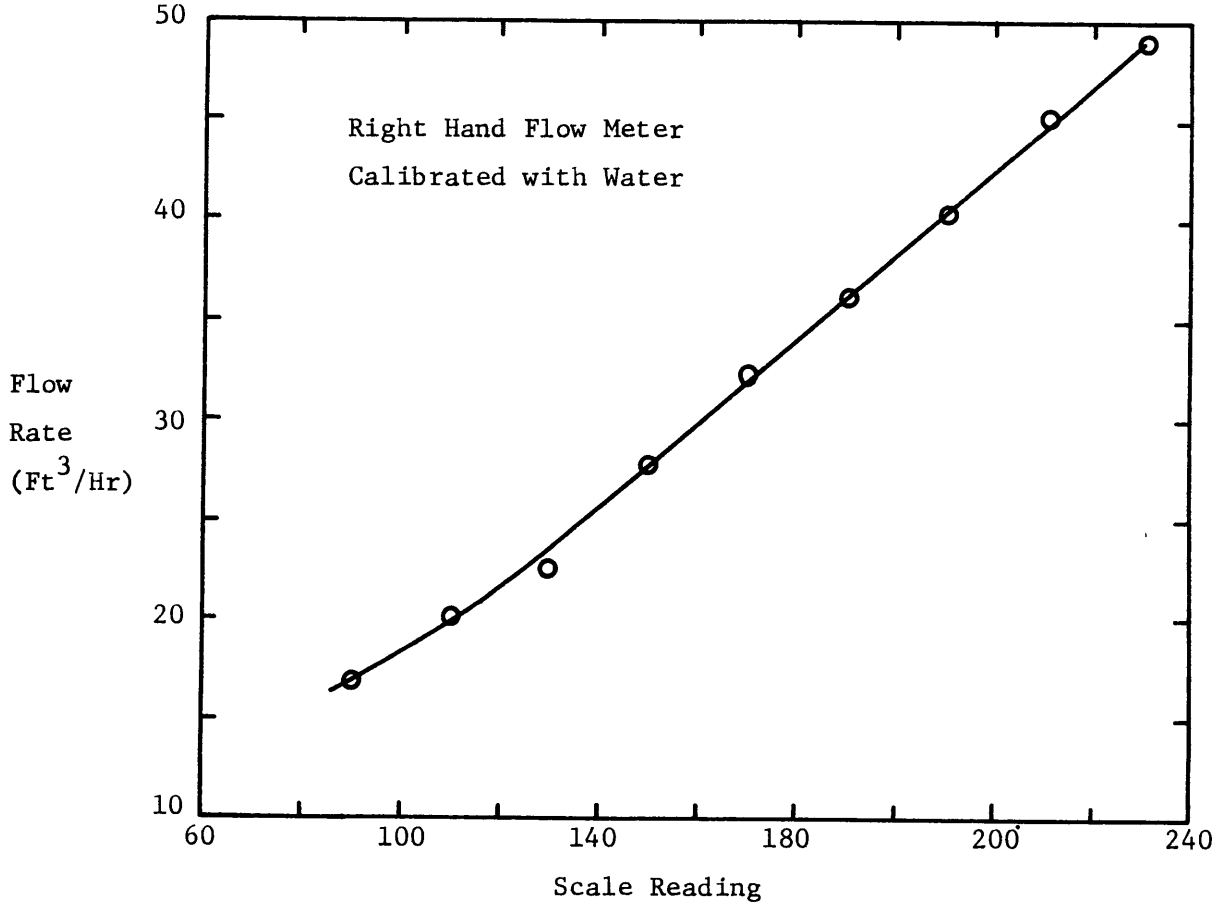

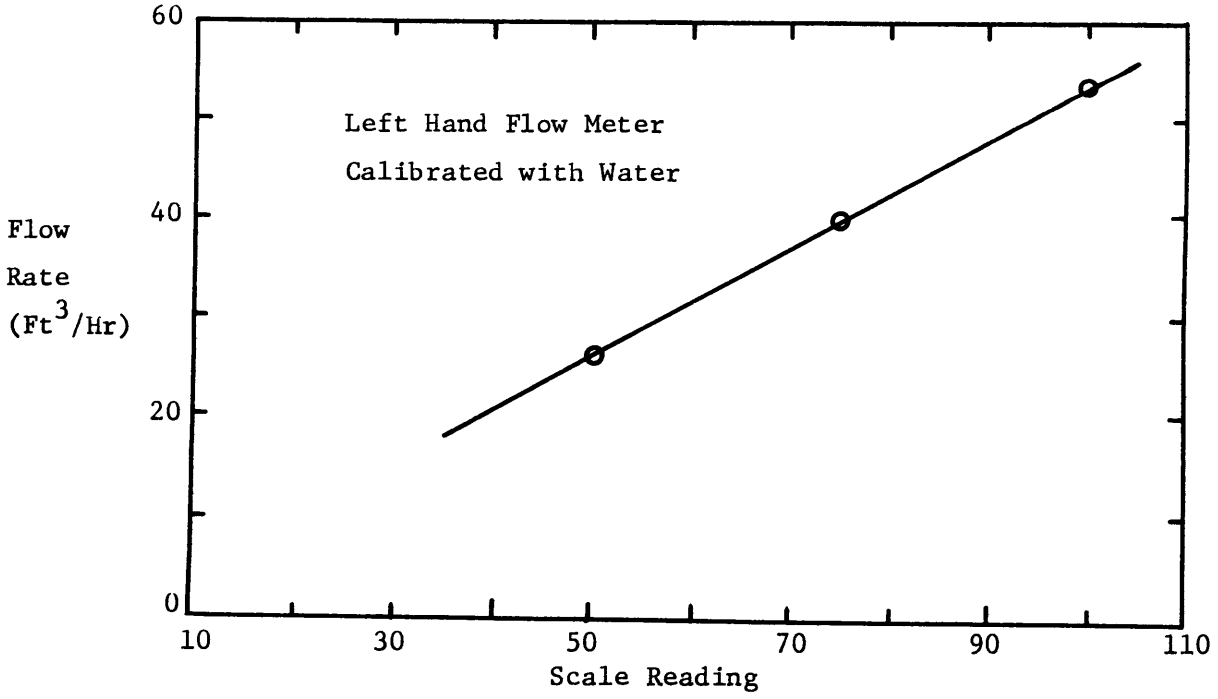

FIGURE 10

TRANSIENT WALL TEMPERATURE PROFILES AT COLLAPSE

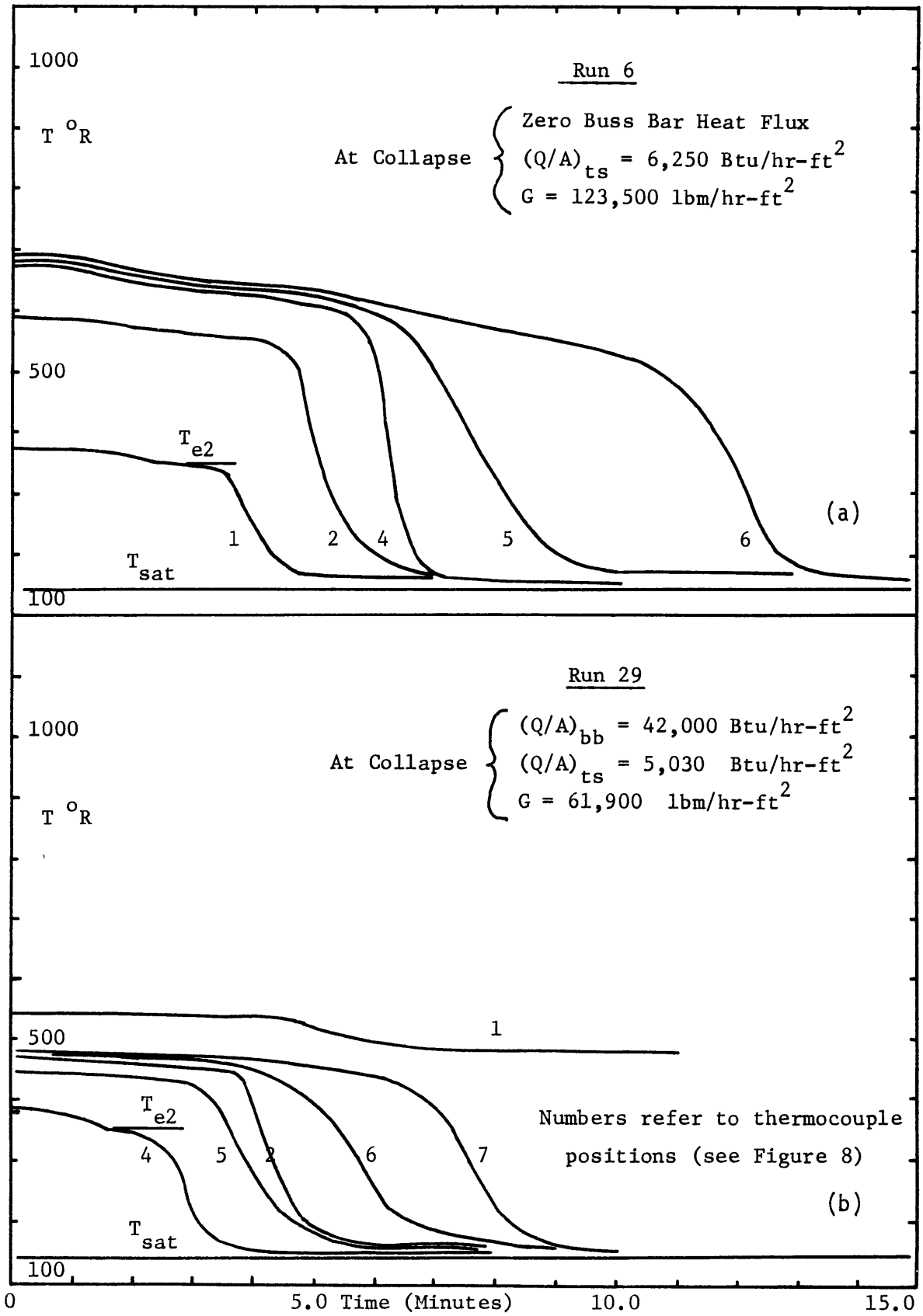

FIGURE 11

POSITION OF START OF VAPOR FILM
RELATIVE TO TEST SECTION

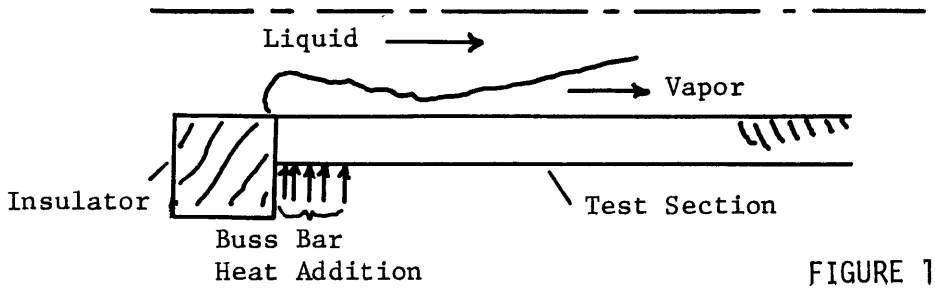

FIGURE 12

TEMPERATURE PROFILE IN VICINITY OF
POINT OF DISCONTINUITY

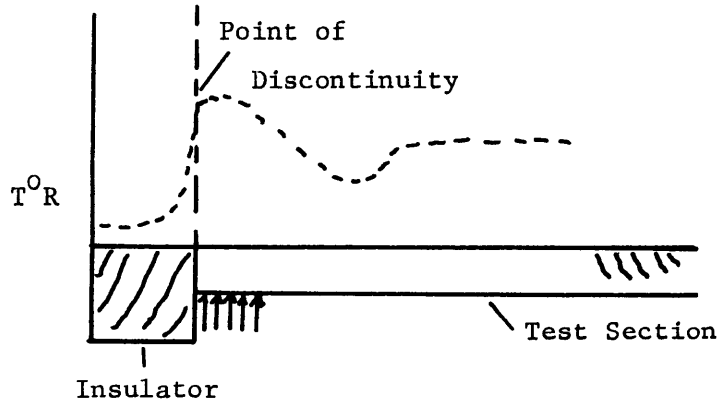

FIGURE 13a

MODEL FOR SOLUTION OF FILM BOILING
COLLAPSE AT ENTRANCE

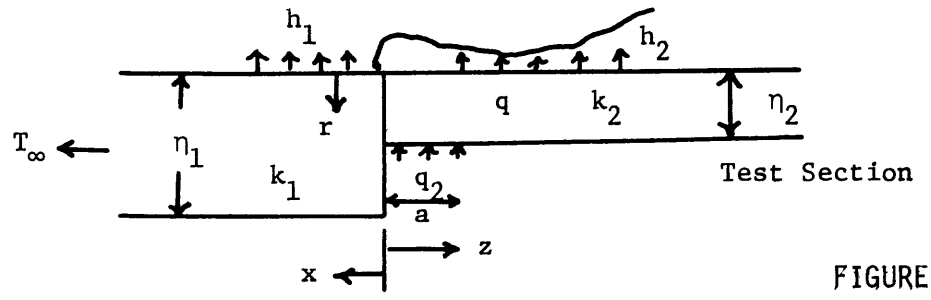

FIGURE 13b

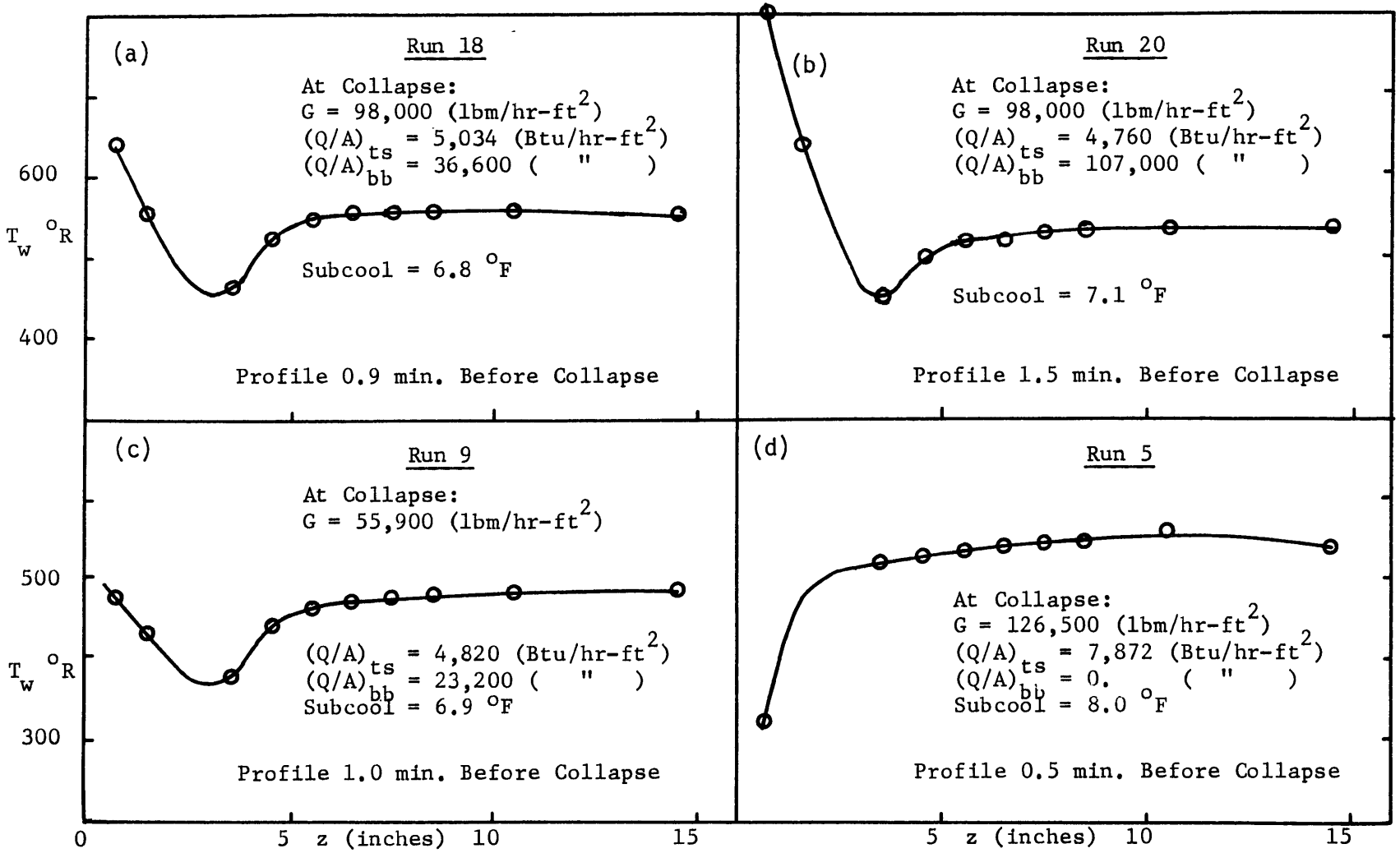

WALL TEMPERATURES BEFORE COLLAPSE
FIGURE 14

PROPAGATION OF COLLAPSE

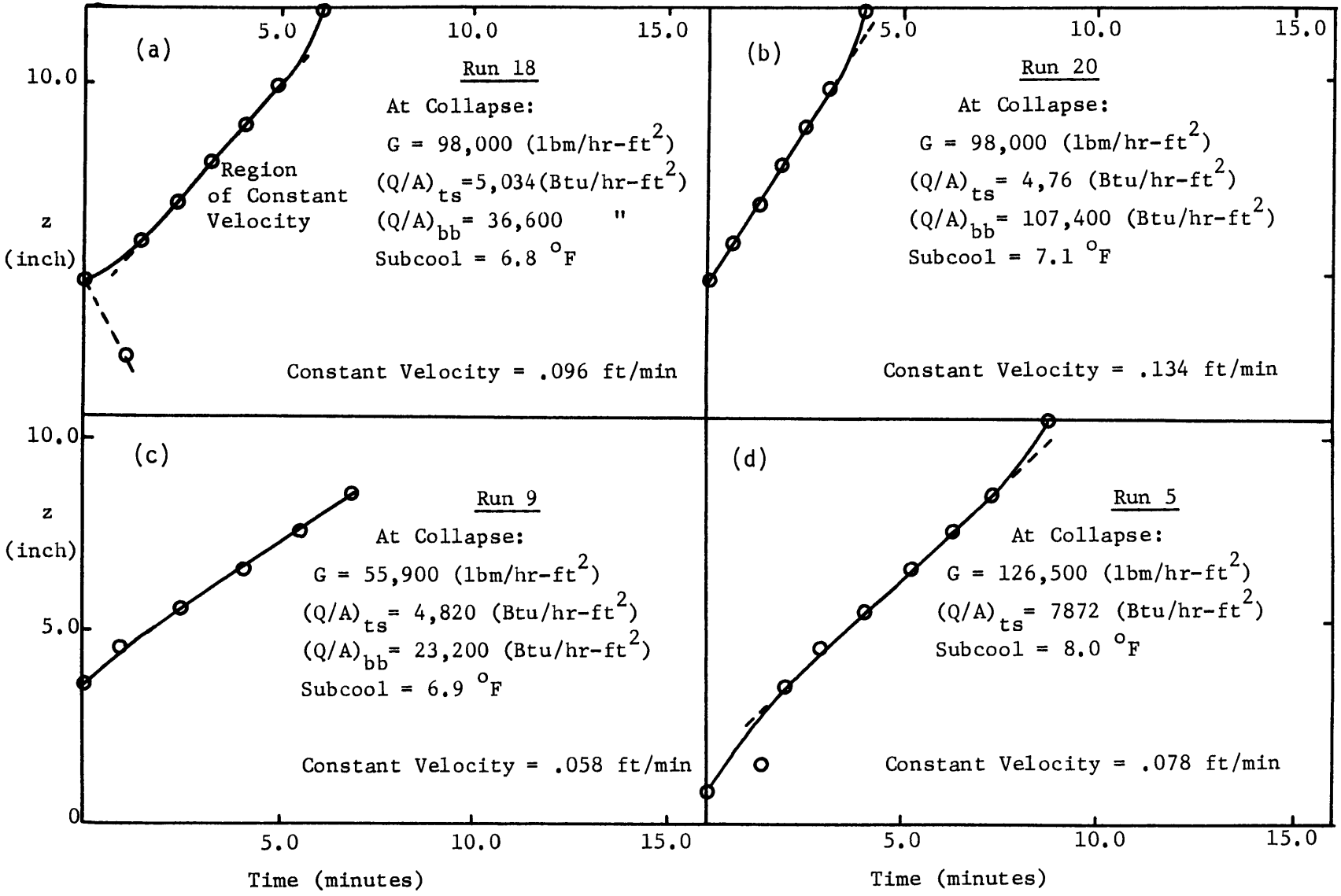

FIGURE 15

COLLAPSE HEAT FLUX VS $(Q/A)_{bb}$
AT CONSTANT MASS FLUX

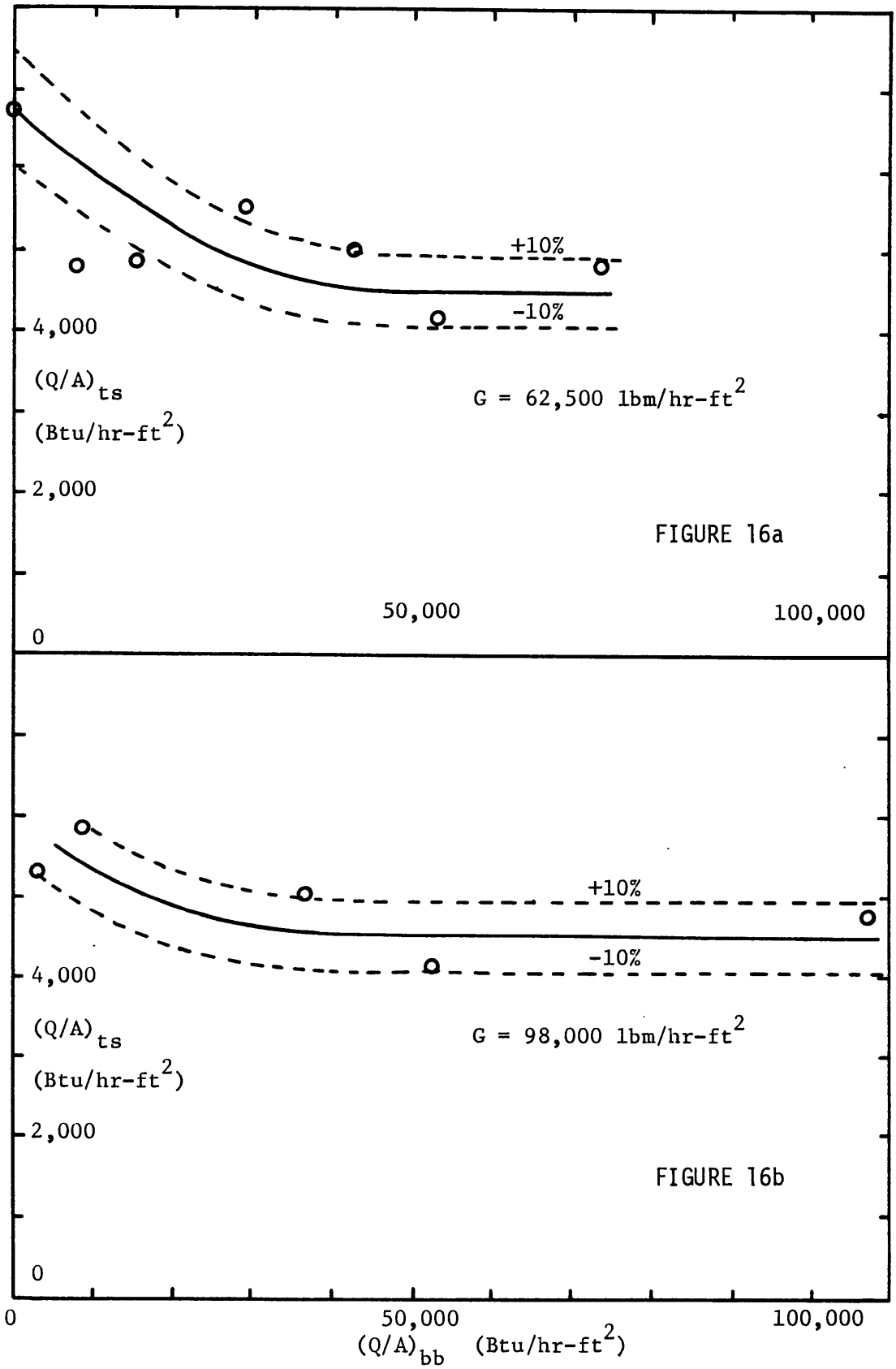

FIGURE 16a

FIGURE 16b

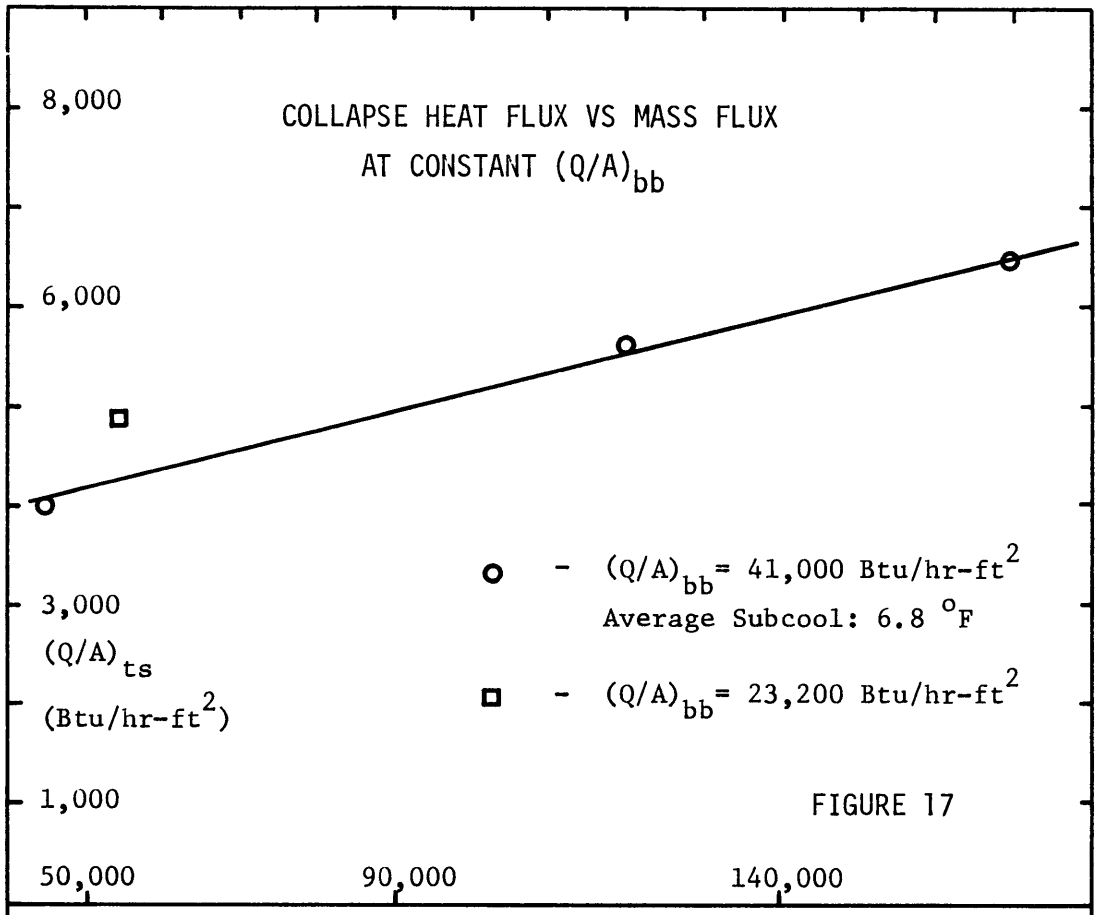

FIGURE 17

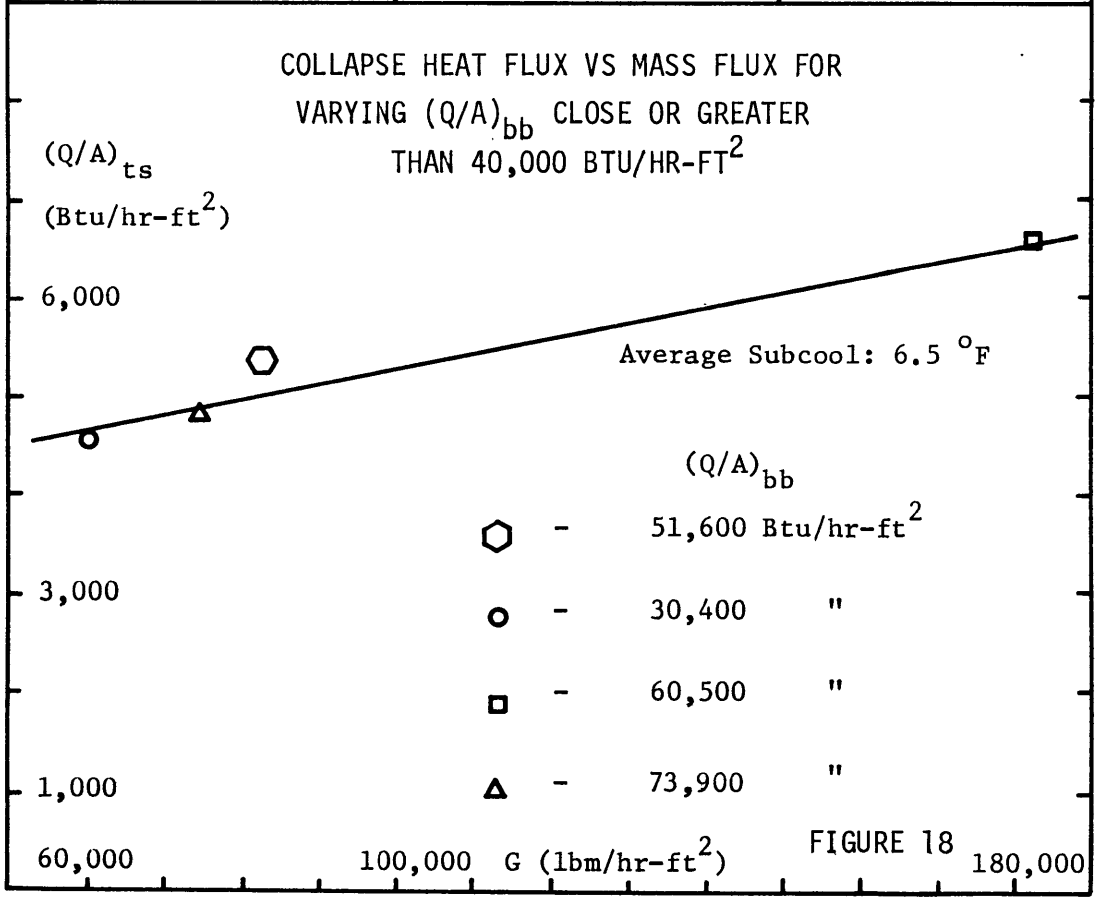

FIGURE 18

COLLAPSE TEMPERATURE DIFFERENCE ($T_w - T_s$) VS MASS FLUX

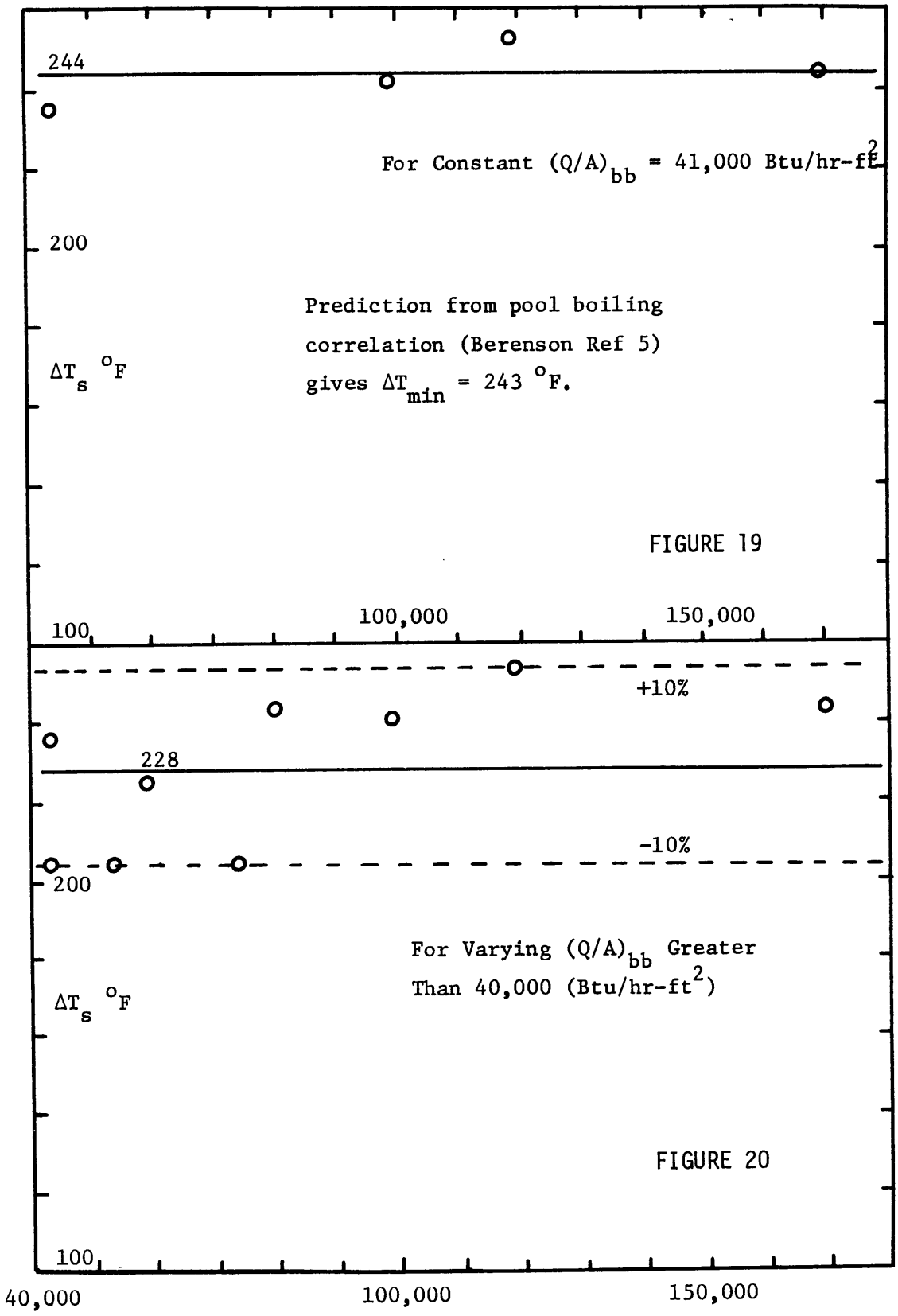

FIGURE 19

FIGURE 20

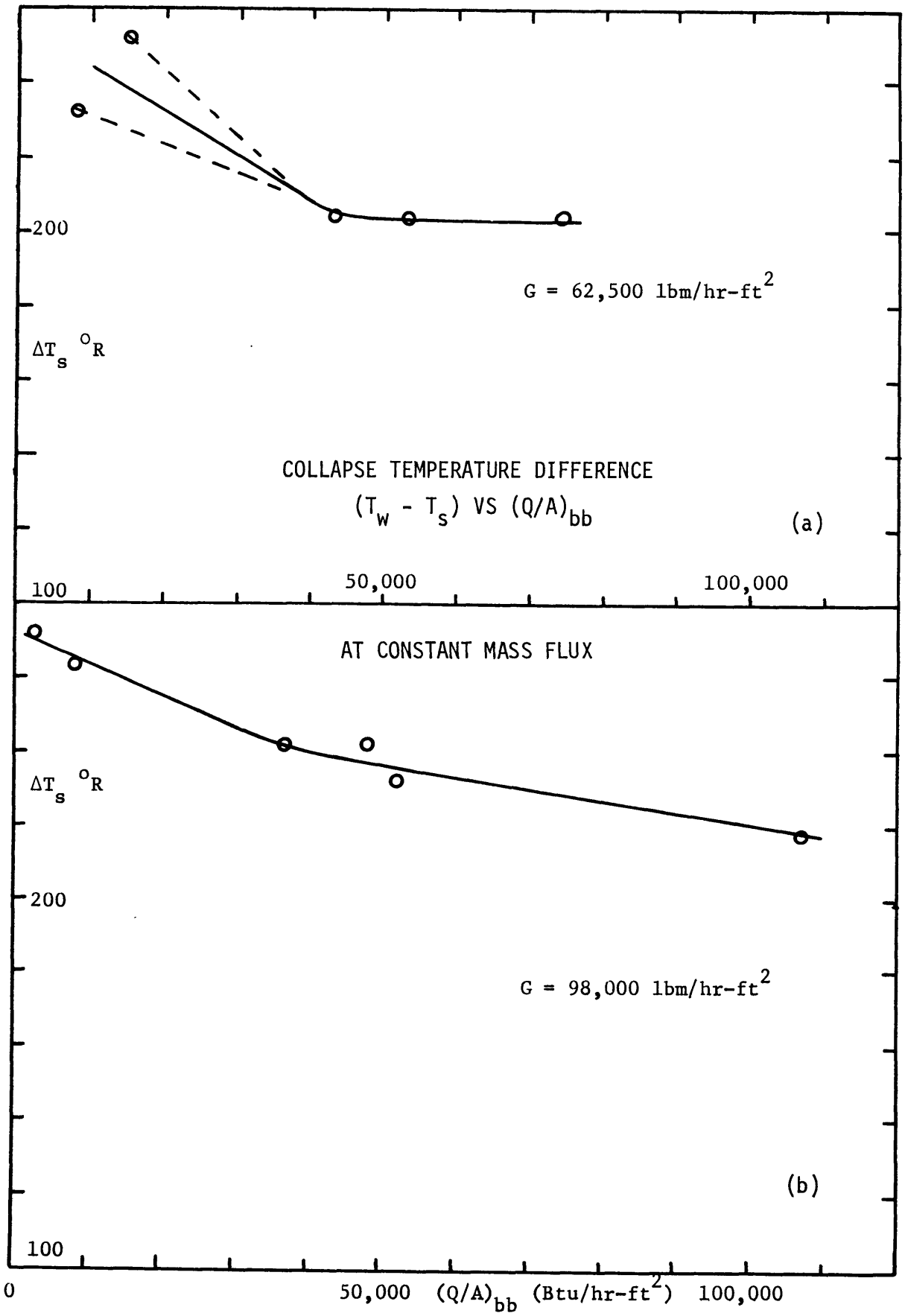
200
ΔT_s °R
G = 62,500 lbm/hr-ft^2
COLLAPSE TEMPERATURE DIFFERENCE
$(T_w - T_s)$ VS $(Q/A)_{bb}$
(a)
100
50,000
100,000
AT CONSTANT MASS FLUX
ΔT_s °R
200
G = 98,000 lbm/hr-ft^2
(b)
100
0
50,000 $(Q/A)_{bb}$ (Btu/hr-ft^2) 100,000

FIGURE 21

COLLAPSE HEAT FLUX VS MASS FLUX
AT ZERO BUSS BAR HEAT FLUX

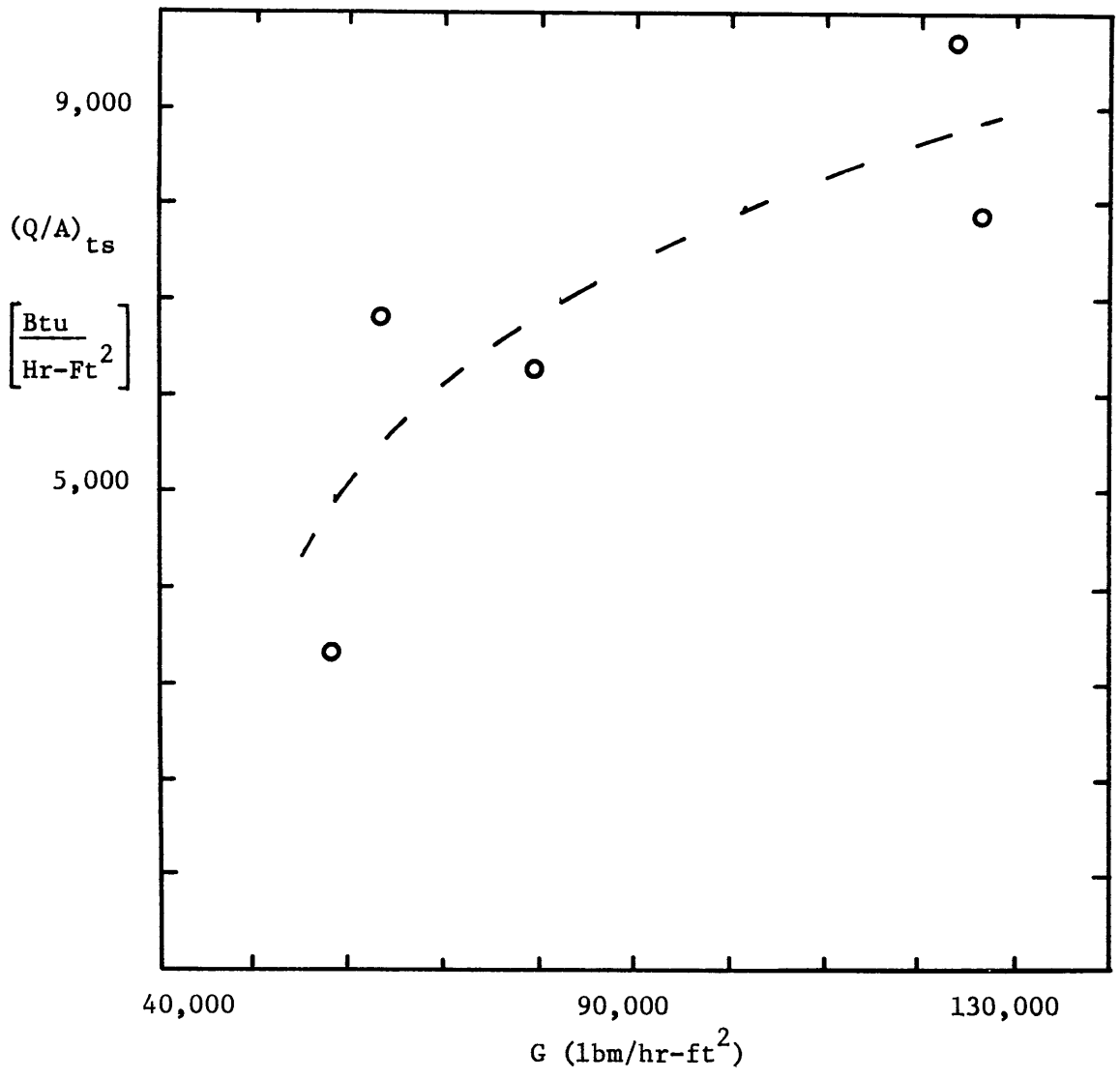

FIGURE 22

◇ Run 16 G = 119,400 lbm/hr-ft^2

□ Run 11 G = 127,750 lbm/hr-ft^2

◇ Run 10 G = 98,000 lbm/hr-ft^2

○ Run 15 G = 186,000 lbm/hr-ft^2

△ Run 8 G = 43,000 lbm/hr-ft^2

--- Pool Boiling Data for Liquid Nitrogen ref (10)

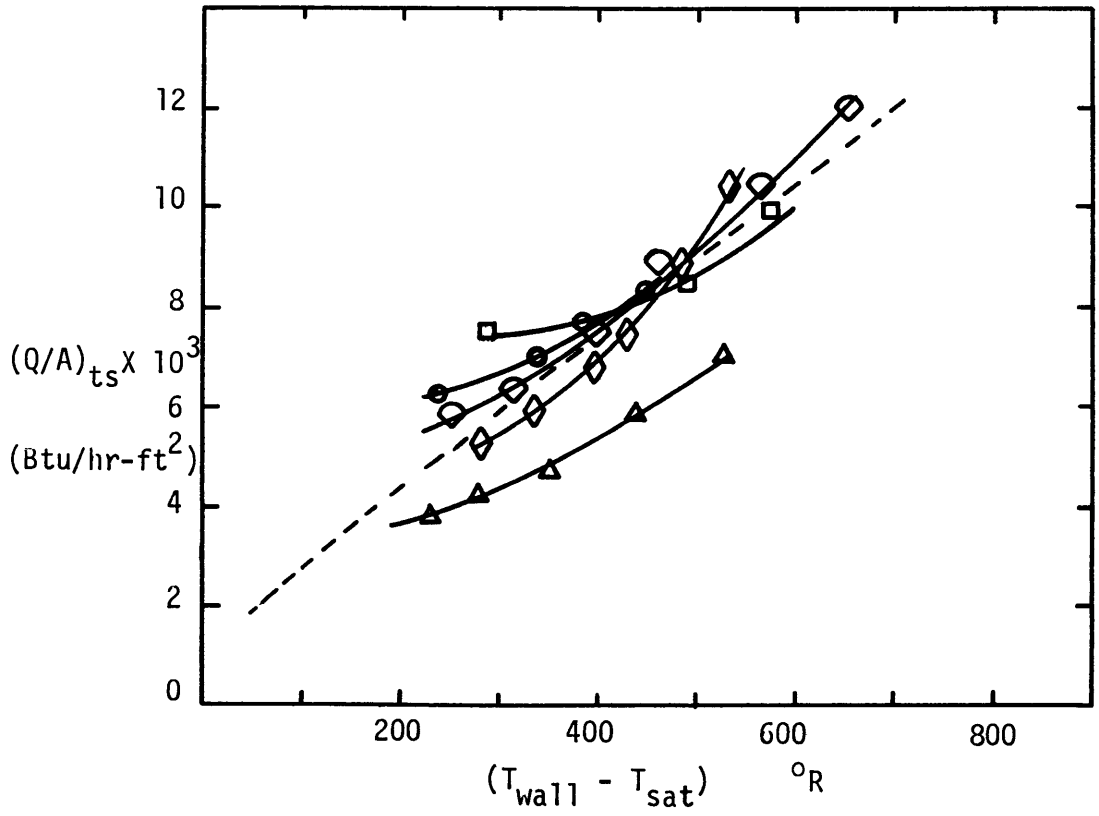

Q/A VS $(T_w - T_{sat})$ FOR THERMOCOUPLE 4

FIGURE 23

TEST SECTION INSULATION RESISTANCE

VS

$(T_{wall} - T_{ambient})$

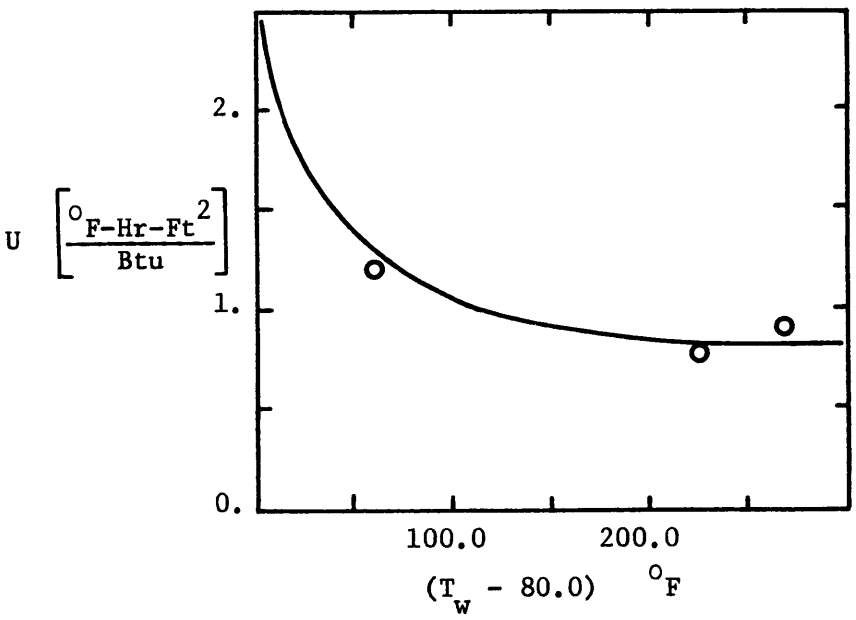

FIGURE 24

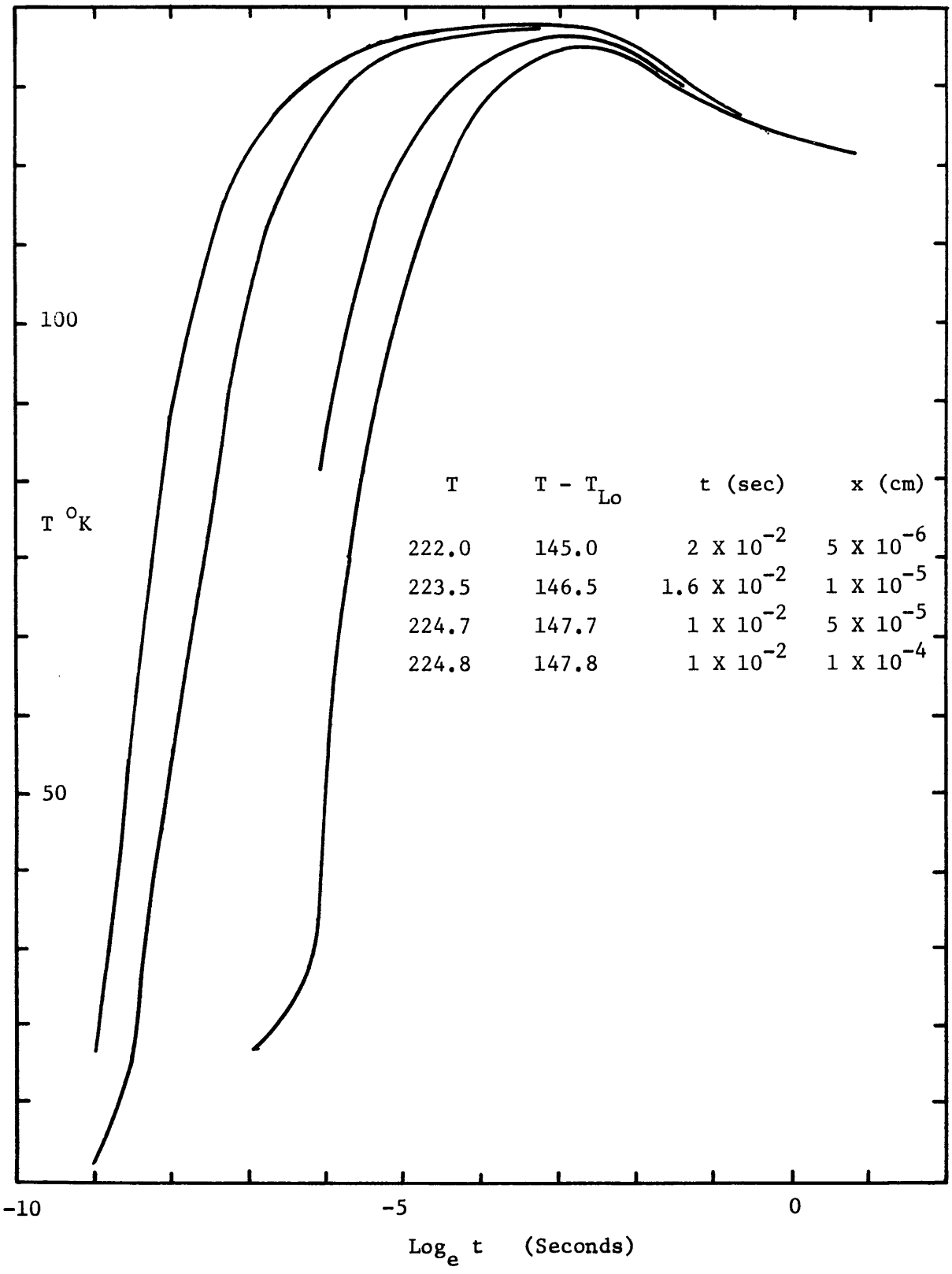

T	T - T_{Lo}	t (sec)	x (cm)
222.0	145.0	2×10^{-2}	5×10^{-6}
223.5	146.5	1.6×10^{-2}	1×10^{-5}
224.7	147.7	1×10^{-2}	5×10^{-5}
224.8	147.8	1×10^{-2}	1×10^{-4}

TEMPERATURE VARIATION WITH TIME IN LIQUID AT VARIOUS DISTANCES FROM THE WALL

FIGURE 25